Université du Québec
Institut National de la Recherche Scientifique
Centre Énergie Matériaux Télécommunications

Low-dispersion, broadband two-wire waveguide for THz and its application

by

Manoj Kumar Mridha

Mémoire ou thèse présentée pour l'obtention du grade de
Maître ès sciences (M.Sc.)

Jury d'évaluation

Président du jury et examinateur interne	Prof. Patrizio Antici INRS-EMT
Examinateur externe	Prof. Arkady Major Department of Electrical and Computer Engineering University of Manitoba
Directeur de recherche	Prof. Roberto Morandotti INRS-EMT
Codirecteur de recherche	Prof. François Vidal INRS-EMT

© Droits réservés de *(Manoj Kumar Mridha)*, 2014

Acknowledgements

I am very grateful to my supervisors Prof. Roberto Morandotti and Prof. François Vidal for guiding me throughout my Master's program. Without their support, collaborations and vision, it wouldn't have been possible to finish my Master. I am immensely thankful for their generosity for funding my Master and allowing me to participate in several national and international conferences.

I would specially like to thanks Dr. Matteo Clerici and Dr. Anna Mazhorova who were always there to discuss ideas with me, help me in my experiments and in moving my project forward. They have been my mentors and I am very pleased to have learned from their invaluable experience and expertise.

I am very thankful to all the members of the Ultrafast Optical Processing Group for giving their invaluable suggestions and inputs whenever I needed it. I would also take this opportunity to thank Mr. Robin Helsten, Dr. Xavier Ropagnol, Mr. Maxime Daneau and Mr. Pierre-Luc Lavertu for their support during my Master.

My heartiest thanks also goes to the staff members of INRS-EMT's administration, who were very helpful and supportive.

Last but not the least, I am immensely thankful to my endless list of friends in Montreal, who gave me the comfort of a family in an unknown country. They cheered me up and gave me the emotional strength to pass through some of my tough times here.

Finally, I would like acknowledge my lovely parents and dear sister for their love and support. I admire their patience and sacrifice for allowing me to stay far away from them, in order to follow my dreams.

Abstract

Terahertz (THz) radiation (0.1-10 THz) is a part of the electromagnetic spectrum lying in between the electrical domain of microwaves and the optical domain of infrared radiation. For the last two decades, this region has been regarded to as a gap due to the lack of sources and detectors. With the development in semiconductor and photonic technologies, several sources and detectors are now becoming available for THz radiation. As a result, THz gap is vanishing and this radiation is finding a lot of applications in material characterization, imaging of biological tissues, security check and is stimulating further fundamental investigations on light-matter interaction. Terahertz radiation may play a major role in the future of "communications". Terahertz is indeed higher in frequency than microwaves, and may provide larger bandwidth for transmitting information. The availability of larger bandwidth and higher frequency could significantly increase the data transfer rates with respect to the available microwave based wireless communication system.

In order to propagate the electromagnetic signal required for communications purposes over long distances, guided wave approaches must be developed to counteract the natural diffraction of the radiation. To this end, THz waveguides are extremely important and in this thesis we discuss the possible implementation and the characteristics of a two-wire THz waveguide.

The first part of the thesis discusses the characterization and applications of the metallic two-wire THz waveguide. The waveguide is made up of two copper wires of 125 μm radius each, with a wire separation of 300 μm and over 20 cm of length. It has been demonstrated to carry a low-dispersive Transverse Electromagnetic Mode (linearly polarized TEM) with about 2 THz of bandwidth. The TEM mode can be excited by a Photoconductive (PC) antenna, which emits a linearly polarized beam with a quasi-Gaussian envelope. For the waveguide to carry the TEM mode, the separation between the wires should be close to the wavelength of operation (300 μm in our case). The low-dispersive characteristic, associated with the confinement of the TEM mode between the two wires, opens up new prospects for THz signal processing and enhanced THz-Time Domain Spectroscopy (THz-TDS).

Hence, consistently with the idea of signal processing, we demonstrate spectral filtering in the two-wire waveguide by inserting a polymer Bragg grating in its guiding region. The grating creates a notch of almost 23 dB with a line width of ~16 GHz in the waveguide spectrum

at 0.5823 ± 0.0003 THz. Furthermore, one of the consequences of a notch in the spectrum is the appearance of the "slow-light effect", which is associated with low group velocity at the edge of a resonance. Due to the slow-light effect induced by the polymer grating, a strong enhancement in the water absorption line at 0.557 THz was observed.

Finally, the possibility of increasing the coupling of the THz signal into the two-wire waveguide was investigated. This was done by generating the THz radiation directly inside the waveguide. A piece of GaAs with breadth and width equal to the separation between the two wires was inserted in between the wires. The combination of voltage applied to the wires (as the electrodes) and the femtosecond laser pulse focused onto the GaAs piece (as the semiconductor) allowed the system to behave like a PC antenna and a THz transmitter. The peak amplitude measured in this configuration was five times larger than the peak amplitude measured when the waveguide was coupled to an external PC antenna for similar excitation power and applied voltage.

Résumé en français

1. Introduction

La radiation térahertz (THz) est un rayonnement électromagnétique qui se situe entre 0.1 et 10 THz, entre le domaine électrique des micro-ondes et le domaine optique du rayonnement infrarouge lointain. Typiquement, le rayonnement à 1 THz possède une longueur d'onde de 300 μm, un nombre d'onde de 33 cm^{-1}, et une énergie des photons de 4.1 meV. La Fig. 1 montre la position du rayonnement THz dans le spectre électromagnétique.

Cette gamme de fréquence était également connue comme la « lacune THz » en raison du manque de disponibilité de sources et de détecteurs performants dans cette région. Grâce à la croissance et au développement rapides dans le domaine de l'optique ultra-rapide et de la physique des semi-conducteurs, la « lacune THz » est en train de se remplir. Plusieurs types de détecteurs et de sources ont été développés au cours des deux dernières décennies. Cela comprend : des sources continue (CW) telles que les « photomixers » [1], les « Backward Wave Oscillators » (BWO) [2], les lasers à gaz dans l'infrarouges lointain [3], les lasers à cascade quantique [4], etc., ainsi que des détecteurs tels que les cellules de Golay, les détecteurs pyroélectriques [5], etc. Des sources THz pulsées à large bande et des détecteurs ont également été développées. Cela comprend : les antennes photoconductrices (PC) [6], les cristaux électro-optiques [7], les plasmas d'air [8], etc. Avec le développement de sources et de détecteurs performants, le rayonnement THz a rapidement attiré l'attention de la communauté de la recherche en raison de ses propriétés uniques. Le rayonnement THz peut facilement passer à travers des matériaux diélectriques tels que le papier [9], le tissu [10], le bois [11] et les

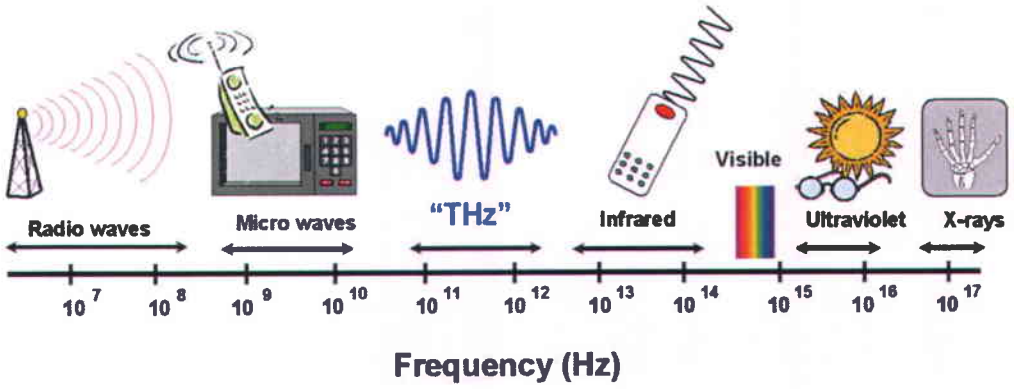

Fig.1 Spectre électromagnétique [12]

matières plastiques [13], à la différence du rayonnement infrarouge qui est absorbé par ces matériaux. Il est également plus court en longueur d'onde que le rayonnement micro-ondes, ce qui fait du rayonnement THz un très bon candidat pour imager des structures diélectriques avec une résolution de l'ordre du millimètre ou même meilleure. En raison de la faible énergie des photons THz (4.1 meV à 1 THz), le rayonnement THz est non-ionisant et ne représente pas de risques pour la santé des tissus vivants et des êtres humains, contrairement aux rayons X. Par conséquent, le rayonnement THz peut être utilisé par exemple pour l'imagerie biomédicale des tissus [14] basée sur l'information obtenue sur leur teneur en eau. Concernant les objets extraterrestres, le rayonnement THz fait partie inhérente de leur émission de corps noir. De plus, la présence de composés spécifiques apparaît dans les spectres de rotation et de vibration à des fréquences THz [15]. On peut imaginer que la spectroscopie THz pourrait être utilisée pour détecter la présence de vie extraterrestre dans le futur.

L'une des principales applications du rayonnement THz est la spectroscopie THz résolue en temps (« THz-Time Domain Spectroscopy » ou THz-TDS) [16], qui permet d'obtenir l'indice de réfraction complexe du matériau à l'étude. La THz-TDS est utilisée pour étudier la signature spectrale de divers matériaux tels que le papier [9], les polymères [13], les vêtements [10], etc., des explosifs tels que le trinitrotoluène (TNT), le « Research Department Explosives » (RDXs) [17] et de nombreux d'autres composés chimiques dangereux.

Les méta-matériaux (structures complexes artificielles) [18] et les guides d'ondes sont également à l'étude aux fréquences THz. Les méta-matériaux peuvent être utilisés pour modifier le spectre des impulsions THz générées, et les guides d'ondes permettent de transférer le rayonnement THz d'un point à un autre dans l'espace. Les méta-matériaux et les guides d'ondes vont jouer un rôle important dans les applications reliées aux communications et aux senseurs, et sont pour cette raison les sujets traités dans ce mémoire.

2. Motivation et objectifs

Avec une population, des industries, des organisations professionnelles et des infrastructures sans cesse croissantes, il y a une demande persistante pour des taux plus élevés de transfert de données sur de longues distances (réseau de fibre optique) et de courtes distances (réseau sans fil). Afin d'atteindre des taux plus élevés de transfert de données pour les communications sur de courtes distances, la bande passante du système actuel de communication basé sur les micro-

ondes doit être augmentée. Une façon d'augmenter la bande passante de ces systèmes est de passer dans le domaine des fréquences supérieures, c'est-à-dire dans le domaine des THz.

Tout système de communication est construit à partir de plusieurs éléments de base. Il s'agit notamment de sources, des détecteurs, de guides d'ondes et de composants de traitement du signal tels que les méta-matériaux [18] et les réseaux de Bragg [19]. Parmi ces composants, les guides d'ondes vont jouer un rôle essentiel en transférant le signal THz sur de longues distances avec des pertes faibles par rapport à la libre propagation dans l'espace (qui est limitée par la diffraction et l'absorption par la vapeur l'eau ambiante). Les guides d'ondes seront également utiles pour améliorer la THz-TDS. Ces deux domaines auront cependant besoin de guides d'ondes ayant une faible dispersion et une large bande. En outre, la réalisation d'un traitement du signal dans les guides d'ondes mêmes sera un atout supplémentaire pour les futurs réseaux THz. Cela permettrait d'éviter d'utiliser des composants intermédiaires qui peuvent introduire des pertes supplémentaires du signal.

En regard de ce qui précède, l'objectif du travail présenté dans ce mémoire a été de développer un guide d'ondes permettant de propager le signal THz sur de longues distances et d'effectuer un traitement du signal à l'intérieur du guide d'ondes. Le mode TEM confiné étroitement et la faible dispersion du guide d'ondes à deux fils étudié ont permis de réaliser un filtrage de fréquence par l'insertion d'un réseau de polymère entre les fils. De plus, nous avons démontré la possibilité de générer le rayonnement THz à l'intérieur même du guide d'ondes au moyen d'une pièce mince de GaAs insérée entre les deux fils du guide d'ondes, qui joue ainsi le rôle d'une antenne PC.

3. Structure de ce mémoire

Ce mémoire a été divisé en cinq chapitres.

Le chapitre 1 est le chapitre d'introduction qui traite du domaine des THz en général. Il décrit certaines des sources et des détecteurs du rayonnement THz et les divers secteurs où la technologie THz est utilisée ou peut être potentiellement utilisée. Ce chapitre discute ensuite des motivations pour développer des guides d'ondes THz ayant une faible dispersion et une large bande, puis présente une revue de la littérature sur les guides d'ondes THz.

Le chapitre 2 présente une introduction à la théorie des guides d'ondes à deux fils. Il décrit ensuite les résultats d'un modèle théorique du guide d'ondes à deux fils développé et

caractérisé dans ce mémoire. Enfin ce chapitre décrit le montage expérimental utilisé, les résultats obtenus et leur discussion.

Le chapitre 3 décrit une démonstration expérimentale du traitement du signal effectué à l'intérieur du guide d'ondes à deux fils par l'utilisation d'un réseau de polymère. Ce chapitre commence par une brève discussion de la théorie des réseaux de Bragg à fibre, suivie par un compte rendu des travaux antérieurs sur les structures périodiques utilisées pour le rayonnement THz. Il décrit ensuite la structure de polymère utilisée comme un réseau à l'intérieur du guide d'ondes à deux fils, ainsi que les résultats expérimentaux obtenus. La fin de ce chapitre traite de l'amplification de l'une des raies spectrales de l'eau dans le spectre THz. Cette amplification résulte du ralentissement de la lumière causé par le réseau de polymère placé à l'intérieur du guide d'ondes.

Le chapitre 4 contient une étude sur la possibilité de générer un rayonnement THz à l'intérieur même du guide d'ondes en plaçant un mince morceau de GaAs entre les deux fils. La tension mécanique sur ces fils suffit à maintenir la pièce de GaAs en place. Lorsqu'une polarisation électrique est appliquée sur les deux fils et que la pièce de GaAs est illuminée par une impulsion laser, cette pièce joue le rôle d'une antenne PC et génère un rayonnement THz qui se propage dans le guide d'ondes à deux fils.

Le chapitre 5 présente une conclusion à ce mémoire et les perspectives futures.

4. Brève revue de la littérature sur les guides d'ondes

D'une part, de nombreuses structures métalliques ont été étudiées pour guides le rayonnement THz par analogie à celles utilisées pour guider les rayonnements micro-onde et radiofréquence. Ces structures comprennent des plaque parallèles (« Parallel Plate Waveguide » ou PPWG) [20, 21], des guides d'ondes rectangulaires [22] et circulaires [23], des câbles coaxiaux [24], des guides d'ondes composés d'un fil unique [25, 26] et de deux fils [27, 28]. D'autre part, le rayonnement THz étant à proximité de fréquences optiques, telles que le rayonnement infrarouge lointain et l'infrarouge, plusieurs guides d'ondes à base de matériaux diélectriques ont également été étudiés. Pour en citer quelques-uns: des guides d'onde à ruban diélectrique [29], des fibres de saphir [30], des fibres à cristaux photoniques en plastique [31], des fibres sous-longueur d'onde [32, 33], et d'autres. Plusieurs structures composites à base de matériaux diélectriques et métalliques [34, 35] ont également été étudiées.

Les guides d'ondes à base de matériaux diélectriques ne sont pas adaptés pour le transfert du rayonnement THz sur de longues distances ni pour les mesures de THz-TDS. Cela est dû à l'importance de la dispersion et de l'atténuation des impulsions THz dans ces matériaux. Cependant les guides d'ondes métalliques, tels que les PPWG, les guides d'ondes à un fil et à deux fils peuvent transporter des impulsions THz avec une dispersion de la vitesse de groupe (« Group Velocity Dispersion » ou GVD) négligeable. Parmi ces trois guides d'ondes, le guide d'ondes à deux fils comporte le plus d'avantages. D'une part, il peut transporter le rayonnement THz avec un confinement dans les deux directions transverses, contrairement au PPWG où les pertes par diffraction dans la dimension non guidée sont inévitables [36]. D'autre part, les guides d'ondes à deux fils subissent moins de pertes de flexion par rapport aux guides d'ondes à fil unique [36]. En raison des nombreux avantages des guides d'ondes à deux fils, la poursuite du développement de ce type de guides d'ondes est donc impérieuse. Les prochaines sections de ce résumé décrivent les propriétés du guide d'ondes à deux fils et les expériences menées dans le cadre de ce mémoire.

5. Théorie du guide d'ondes à deux fils

Le guide d'ondes à deux fils a été étudié théoriquement pour le guidage du rayonnement THz [27] et expérimentalement pour des fréquences inférieures au GHz [36]. Le schéma de base du guide d'ondes à deux fils, avec des fils de rayon R et de séparation S, est représenté à la Fig. 2. Le mode guidé se trouve dans le plan x-y et se propage dans la direction z. Un guide d'ondes à deux fils transporte un mode TEM faiblement dispersif lorsque S est proche de la longueur d'ondes de fonctionnement. Les caractéristiques de faible dispersion et de fort confinement dans ce guide d'ondes conviennent parfaitement aux études de phénomènes non linéaires dans le régime THz.

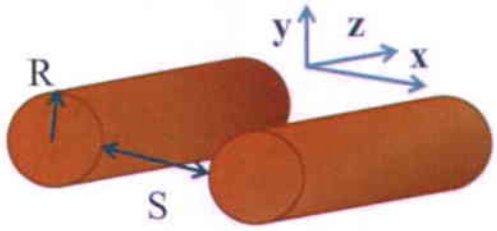

Fig. 2 Schéma d'un guide d'ondes à deux fils avec une séparation S et un rayon R. Le mode guidé se trouve dans le plan x-y et se propage dans la direction z.

Les études théoriques sur le guide d'ondes à deux fils démontrent la différence entre un mode TEM et le mode de Sommerfeld qui existe autour d'un seul fil. La distribution du mode dans la géométrie des deux fils, étudiée dans la référence [27], a été simulée de nouveau ici pour différentes séparations S des fils à une fréquence de 1 THz (longueur d'onde de 300 µm) et pour des fils ayant un rayon R =125 µm. On observe à la Fig. 3 que, pour la séparation S = 300 µm entre les fils (Fig. 3 (a)), le mode TEM est concentré dans l'espace entre les fils. Pour une séparation un peu plus grande que la longueur d'onde (S = 500 µm, Fig. 3 (b)), le mode TEM existe toujours, mais avec un champ électrique concentré plus près des surfaces métalliques. Pour une plus grande distance entre les fils (S = 1500 µm, Fig. 3 (c)), le guide d'ondes à deux fils ne contient plus le mode TEM pour la longueur d'onde de fonctionnement. Il tend maintenant à contenir un mode de Sommerfeld de polarisation azimutale (ou radiale) localisé près de chaque fil. On voit que pour obtenir un mode TEM entre les deux fils, l'écartement entre les deux fils doit être proche de la longueur d'onde de fonctionnement.

6. Le guide d'ondes à deux fils étudié expérimentalement

Cette section du résumé décrit le guide d'ondes à deux fils étudié dans le cadre de ce mémoire. Comme montré à la Fig. 4, une plaque métallique de base fait office de colonne vertébrale à la structure du guide d'ondes. Deux plaques de polymère ont ensuite été attachées à chaque extrémité de la plaque métallique de base. Un trou d'un diamètre de 800 µm a été foré à travers

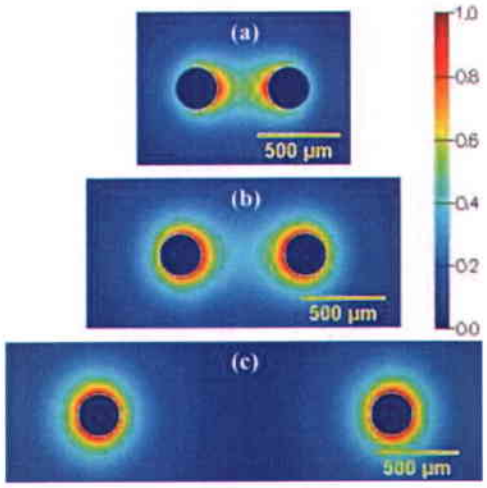

Fig. 3 Distribution du mode dans un guide d'ondes à deux fils pour des fils de 125 µm de rayon et pour des séparations des fils de (a) 300 µm, (b) 500 µm et (c) 1500 µm.

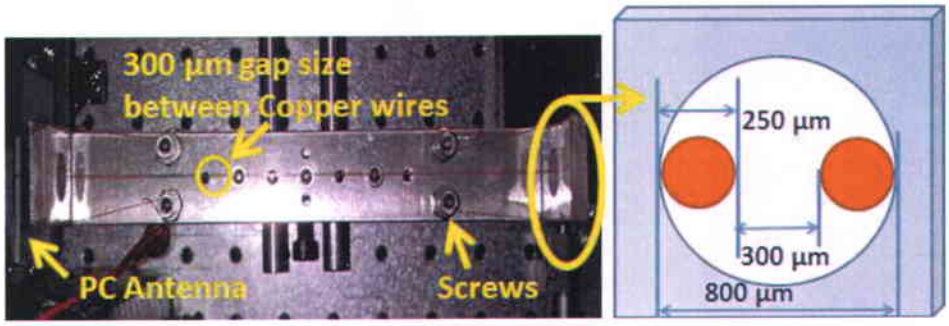

Fig. 4 Conception du guide d'ondes à deux fils avec le dispositif permettant d'obtenir une séparation de 300 µm.

les plaques de polymère. Les deux fils ont ensuite été passés à travers les trous. Les quatre extrémités libres des fils ont ensuite été attachées aux quatre vis fixées à la plaque de base. Ces vis ont permis de tendre les fils et ainsi les maintenir avec un espacement uniforme. Comme les trous avaient un diamètre de 800 µm et que chacun des fils avait un diamètre de 250 µm, une séparation de 300 µm entre les fils a été obtenue. La longueur totale du guide d'ondes à deux fils était de 20 cm.

7. Description du montage expérimental

Le dispositif expérimental utilisé pour caractériser le guide d'ondes à deux fils est basée sur le principe de la THz-TDS tel que représenté à la Fig. 5. La source laser Ti-saphir femtoseconde utilisée possède un taux de répétition de 80 MHz et une durée d'impulsion de 125 fs. Le faisceau laser provenant du laser femtoseconde est ensuite divisé en deux parties: la pompe et de la sonde. Le faisceau pompe transporte environ 150 mW de puissance et le faisceau de sonde, une puissance inférieure à 10 mW.

Le faisceau pompe est dirigé dans la partie de génération du rayonnement THz et le faisceau sonde, dans la partie de détection du rayonnement THz. Le rayonnement THz est généré à partir d'une antenne PC dont la fente a une largeur de 120 µm entre les électrodes. L'antenne PC est polarisée à 60 V avec une tension électrique en forme d'onde carrée et génère un rayonnement THz lorsque le faisceau pompe est focalisé sur celle-ci. Le système de détection THz est basé sur une technique de détection électro-optique et est constitué par un cristal de ZnTe, d'une plaque quart d'onde (QWP), d'un prisme de Wollaston et d'une paire de photodiodes, qui sont connectées à un amplificateur de verrouillage. Deux miroirs paraboliques,

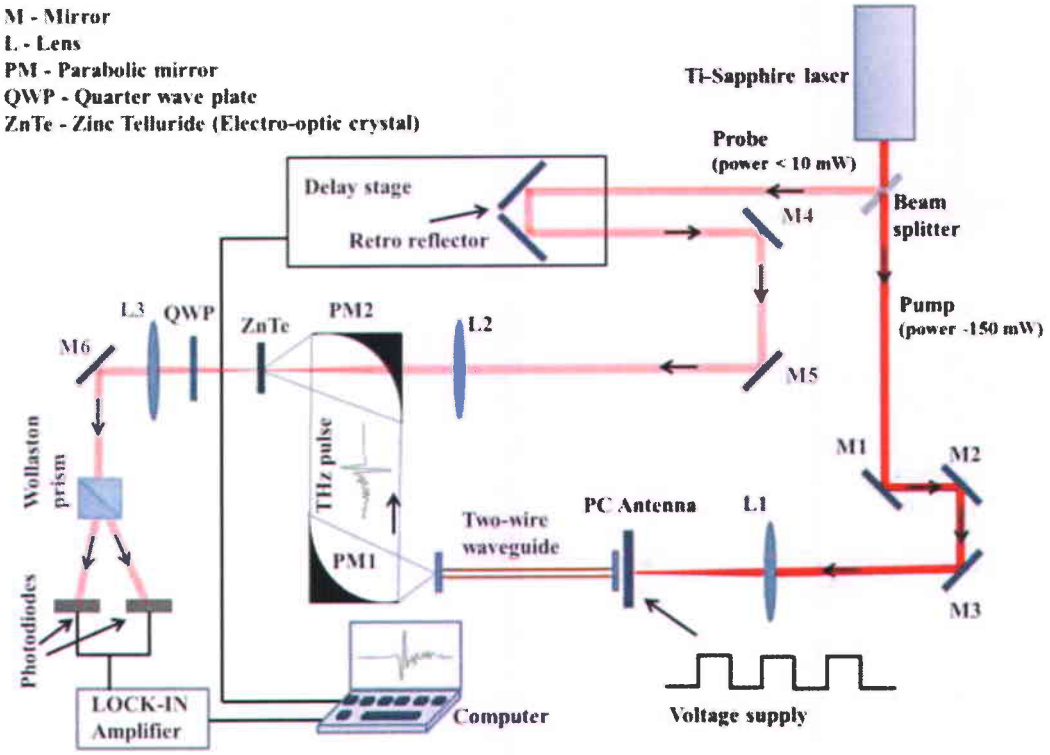

Fig. 5 Schéma expérimental utilise pour la caractérisation du guide d'onde.

PM1 et PM2, sont utilisés pour collecter le rayonnement THz et le focaliser sur le cristal de ZnTe. Un ordinateur lit le signal THz de l'amplificateur de verrouillage et contrôle la ligne à délai.

Dans notre dispositif expérimental, le système de détection est fixe. Donc, afin de mesurer le signal généré par l'antenne PC, celle-ci est placée au foyer de PM1. De même, afin de détecter le signal transporté dans le guide d'onde de 20 cm, l'extrémité de sortie du guide d'ondes est placée au foyer de PM1. Afin de coupler efficacement le rayonnement THz généré par l'antenne avec le guide d'ondes, l'antenne est placée très près de l'extrémité d'entrée du guide d'ondes, comme illustré à la Fig. 5.

8. Résultats et discussion sur le guide d'ondes à deux fils

Les expériences sur le guide d'ondes à deux fils ont été effectuées dans un environnement purgé (azote à 0% d'humidité). Les résultats expérimentaux montrent une propagation du rayonnement THz faiblement dispersive et à large bande à travers le guide d'ondes. Le signal temporel de référence (i.e. le signal généré par l'antenne PC) et les spectres de puissance de l'impulsion sont

représentés respectivement sur les Fig. 6 (a) et 6 (b). De même, le signal temporel THz après propagation dans le guide d'ondes et spectra de puissance correspondante sont représentés respectivement sur les Fig. 6 (c) et 6 (d). En comparant les Fig. 6 (a) et 6 (c), on observe que la nature sub-picoseconde et à cycle unique du signal de référence est préservée après propagation à travers le guide d'ondes. Cela démontre que l'impulsion THz s'est propagée à travers le guide d'ondes sans « chirp » et avec une GVD négligeable. En comparant les Fig. 6 (b) et 6 (d), on peut observer que le guide d'ondes a également transporté avec succès la large gamme de fréquences (> 2 THz) émise par l'antenne PC. Ces résultats démontrent que le guide d'ondes à deux fils peut transmettre des impulsions THz à large bande avec une faible dispersion.

9. Expériences avec des réseaux de Bragg en polymère pour le filtrage de fréquence

La propagation d'un mode TEM faiblement dispersif et étroitement confiné dans le guide d'ondes à deux fils ouvre la possibilité de traiter le signal THz à l'intérieur même du guide

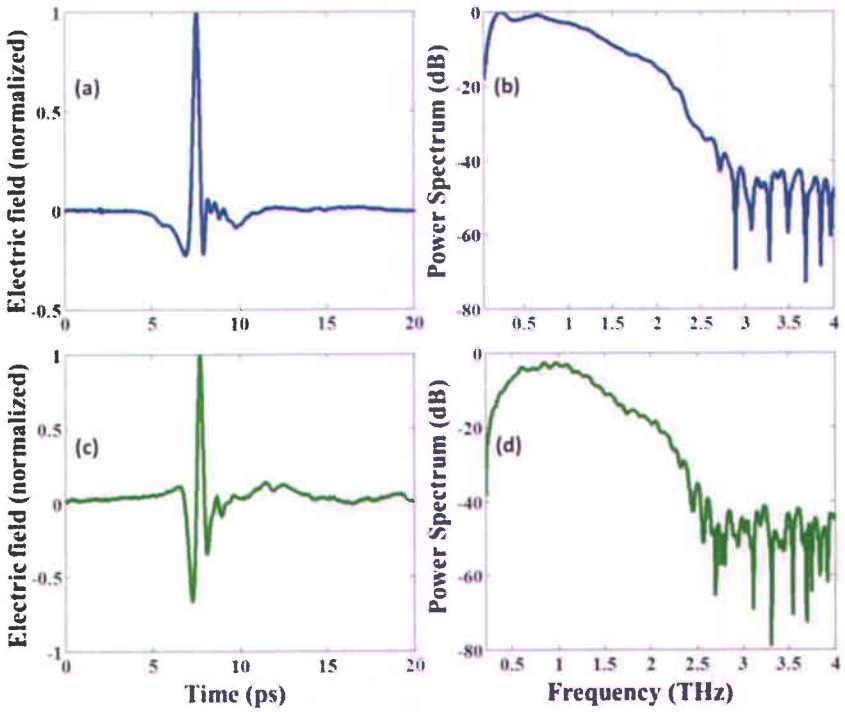

Fig. 6 (a) Signal temporel THz émis par l'antenne PC dans un environnement purgé et (b) le spectre correspondant. (c) Signal temporel THz du guide d'ondes à deux fils de 20 cm dans un environnement purgé et (d) le spectre correspondant. Toutes les courbes ont été normalisées par rapport à leur maximum.

d'ondes. Nous nous sommes particulièrement intéressés au filtrage de fréquence à l'intérieur du guide d'ondes. Pour en effectuer la démonstration, un réseau de Bragg en polymère (polypropylène extrudé), disponible dans le commerce, a été utilisé (voir la Fig. 7 (a)). Le maillage de polymère est constitué de tiges horizontales et verticales dans un mode tissé. Pour utiliser le réseau de polymère comme un réseau de diffraction, les tiges horizontales ont été retirées, comme le montre la Fig. 7 (b). Le diamètre de ces tiges, tel que mesurée au microscope, est de 110 ± 2 μm et l'espacement entre les tiges est de 137 ± 2 μm. Par conséquent, la période du réseau est d'environ 247 μm. Pour l'expérience, 16 périodes du réseau ont été utilisées, ce qui représente une longueur d'environ 4 mm.

Pour l'analyse de ce dispositif, le signal de référence provenant du guide d'ondes seul et le signal après que le réseau ait été inséré dans le guide d'ondes ont été mesurés. Les signaux temporels et le spectre de transmission avec réseau sont représentés respectivement sur les Fig. 8 (a) et 8 (b). Comme on peut l'observer sur la Fig. 8 (a), l'amplitude crête du signal temporel est retardée en raison de l'augmentation de l'indice de réfraction moyen de la structure suite à l'introduction du réseau. La Fig. 8 (b) indique que la perte d'insertion du réseau varie de 1 à 7 dB entre 0.3 et 1 THz. Une fine entaille d'environ 23 dB, avec une largeur de 16 GHz, est observée à 0.5823 THz. Les simulations du type « Finite-Difference Time Domain » (FDTD) du dispositif (en supposant que l'indice de réfraction du polypropylène est 1.51 [13]), a prédit un creux dans le spectre de transmission à 0.5928 THz, avec une largeur de 1.2 GHz, ce qui est en très bon accord avec le résultat expérimental.

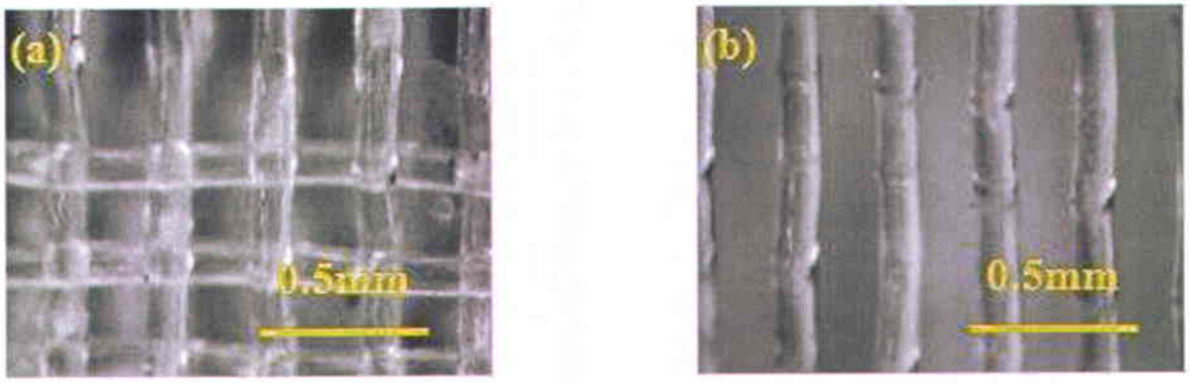

Fig. 7 (a) Le réseau original de polymère composé des tiges horizontales et verticales. (b) Le réseau de polymère une fois que les tiges horizontales aient été retirées.

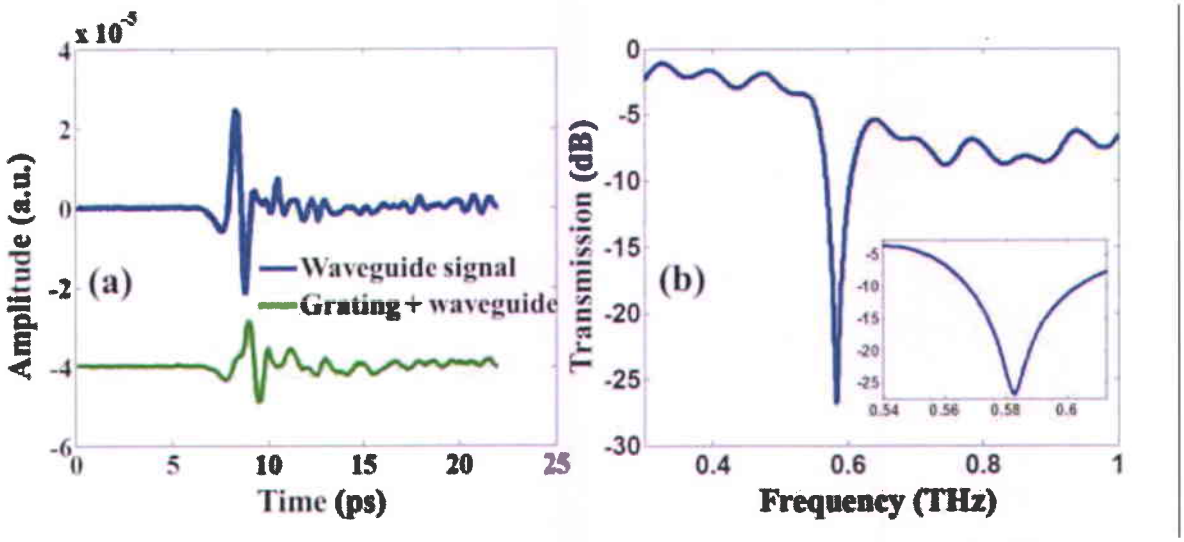

Fig. 8 (a) Signal provenant du guide d'ondes sans (bleu) et avec (vert) le réseau de polymère. (b) Spectre de transmission du signal THz avec le réseau de polymère. Le médaillon montre un vue rapprochée du minimum.

De plus, avec le réseau, nous avons observé une amplification d'une raie de l'eau à 0.557 THz. À la Fig. 9, la courbe rouge représente le spectre du rayonnement THz après propagation dans le guide d'ondes dans un environnement non purgé et en l'absence du réseau. La courbe bleue représente le spectre THz obtenu dans les mêmes conditions mais en présence du réseau. Cette dernière démontre l'amplification de la raie de l'eau à 0.557 THz, laquelle se trouve au bord la bande du réseau. La courbe verte a été mesurée dans les mêmes conditions que la courbe bleue mais dans un milieu purgé (0% d'humidité). Par conséquent, le phénomène observé est sans doute dû à une interaction accrue entre le rayonnement THz et la vapeur d'eau dans l'air ambiant. Il pourrait s'expliquer par le ralentissement de l'impulsion THz se propageant à l'intérieur du guide d'ondes au voisinage de la bande du réseau de Bragg. Par conséquent, après les mises au point nécessaires, ce dispositif pourrait être utilisé comme un senseur d'humidité relative.

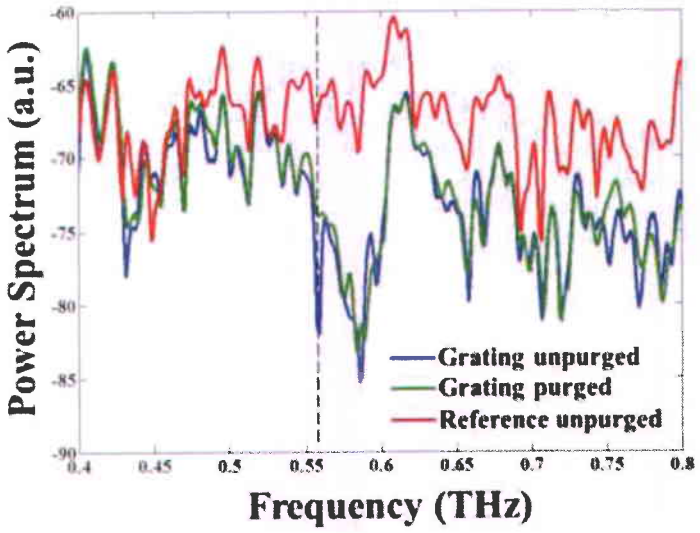

Fig. 9 Courbe bleue: Amplification de la raie de l'eau à 0.557 THz (tirets) dans le guide d'ondes incluant le réseau. Courbe rouge : Spectre obtenu sans le réseau dans les conditions ambiantes (non purgées). Courbe verte : Spectre obtenu avec le réseau dans un environnement purgé.

10. Émetteur THz à deux fils

Cette section traite de la possibilité de générer le rayonnement THz directement à l'intérieur du guide d'ondes à deux fils ou, en d'autres termes, de réaliser un guide d'ondes actif à deux fils (que nous avons nommé « émetteur THz à deux fils »).

Dans les expériences décrites ci-dessus, le rayonnement THz a été couplé avec le guide d'ondes en amenant l'extrémité d'entrée du guide d'ondes très près de l'antenne PC. La réalisation du couplage dans une telle configuration est assez compliquée expérimentalement car il faut aligner le guide d'ondes et l'antenne avec précision. En outre, il faut compter qu'une fraction importante du rayonnement THz généré par l'antenne PC ne soit pas couplée dans le guide d'ondes.

Pour pallier à ces problèmes nous avons imaginé un dispositif où le rayonnement THz serait généré à l'intérieur même du guide d'ondes. Pour fabriquer cet émetteur THz à deux fils, un morceau de GaAs est inséré entre les deux fils de cuivre, comme illustré à la Fig. 10. La pièce de GaAs, qui a une largeur et une épaisseur de 300 µm, est maintenue entre les deux fils tendus. Comme le montre la Fig. 10, le laser pompe est focalisé sur la pièce de GaAs placée à l'extrémité d'entrée du guide d'ondes et une tension électrique est appliquée sur les deux fils formant le

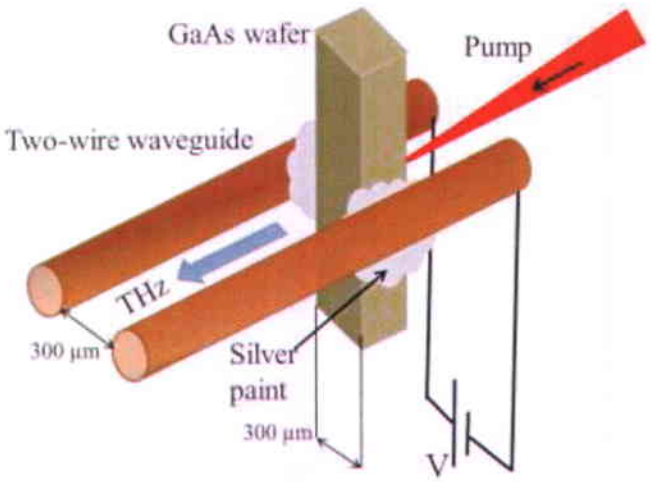

Fig. 10 Schéma du guide d'ondes à deux fils avec génération de rayonnement THz dans le guide d'ondes même (« émetteur THz à deux fils »).

guide d'ondes. Afin d'augmenter l'efficacité de contact entre la pièce de GaAs et les fils de cuivre, une couche de peinture argent est appliquée sur jonction entre les fils et le GaAs. Grâce à l'action combinée de la tension électrique et du laser pompe focalisé sur la pièce de GaAs, le dispositif agit comme une antenne PC. Ainsi, le signal THz généré est directement couplé dans le guide d'ondes à deux fils.

10.1 Résultats expérimentaux et discussion

Pour toutes nos expériences avec l'émetteur THz à deux fils, une puissance du laser pompe de 220 mW a été utilisée et une tension électrique de 110 V a été appliquée sur la pièce de GaAs. Nous avons d'abord démontré que le dispositif agit bien comme une antenne PC. La Fig. 11 montre le signal temporel THz et les spectres de puissance mesurés pour l'antenne seule, sans le guide d'ondes. Ensuite un guide d'ondes à deux fils de 10 cm de longueur a été couplé à cette antenne PC en plaçant l'extrémité du guide d'ondes près de l'antenne, comme dans les expériences décrites ci-dessus (voir la Fig. 12 pour le signal temporel et le spectre). Enfin, la même pièce de GaAs a été insérée entre les deux fils du guide d'ondes de 10 cm (voir la Fig. 13 pour le signal temporel et spectre). Comme on peut le constater sur la Fig. 11, le dispositif s'est comporté comme l'antenne PC utilisée dans les expériences ci-dessus (à la différence que la fente est ici de plus grande taille, soit 300 μm), en délivrant une impulsion THz à cycle unique

sur une largeur de bande de 2 THz. En comparant les Fig. 12 et 13, on observe que le champ du signal crête est cinq fois plus élevé lorsque la pièce de GaAs est insérée dans le guide d'onde que quand l'antenne est placée près de l'extrémité du guide d'ondes. Par conséquent, cette expérience montre que le couplage entre l'antenne PC et le guide d'ondes est beaucoup plus efficace lorsque l'antenne est insérée directement dans le guide d'ondes.

Cependant, on note que la forme de l'impulsion THz produite par l'émetteur THz n'est pas à cycle unique comme prévu. Ces résultats indiquent que l'émetteur THz à deux fils nécessite une étude plus approfondie. Des études théoriques et d'autres expériences devront être menées pour tenter d'améliorer ces résultats expérimentaux préliminaires.

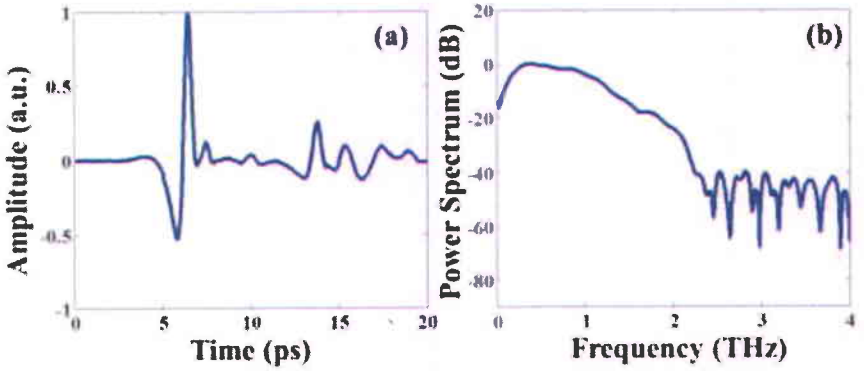

Fig. 11 Signal de la pièce de GaAs utilisée comme antenne PC sans le guide d'ondes: (a) Signal temporel. (b) Spectra de puissance. Les courbes sont normalisées par rapport à leur maximum.

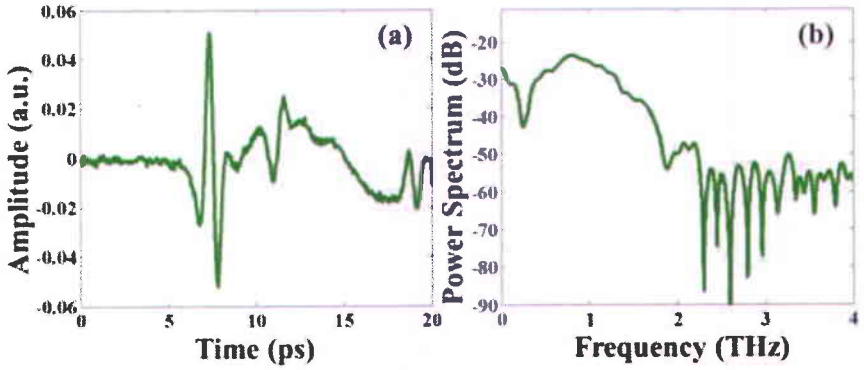

Fig. 12 (a) Signal temporel du guide d'ondes de 10 cm couplé à l'antenne PC composée d'un morceau de GaAs entre deux fils. (b) Spectra de puissance. Les courbes sont normalisées par rapport à leur maximum.

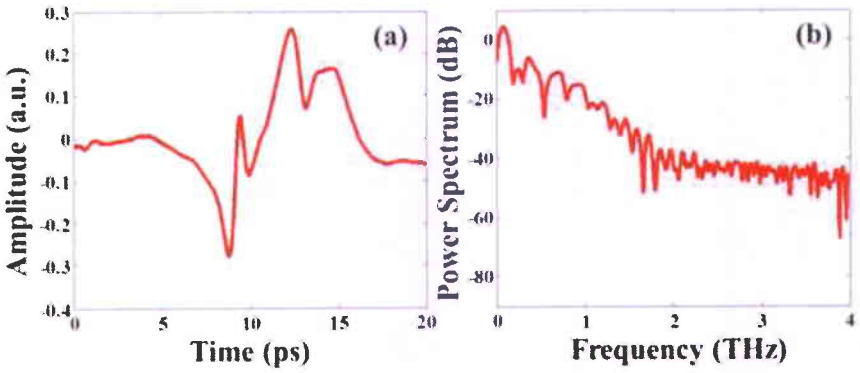

Fig. 13 (a) Signal temporel du guide d'ondes de 10 cm incluant une pièce de GaAs pièce entre les deux fils. (b) Spectra de puissance. Les courbes sont normalisées par rapport à leur maximum.

11. Conclusion et perspectives

L'objectif du travail décrit dans ce mémoire a été de développer un guide d'ondes THz à deux fils métalliques ayant une faible dispersion et une large bande pour les futurs réseaux de communication THz et pour la THz-TDS. Le guide d'ondes à deux fils expérimenté (rayon des fils de 125 µm et séparation de 300 µm) transporte un mode TEM faiblement dispersif lorsque la distance de séparation des fils est comparable à la longueur d'ondes de fonctionnement. Lorsque la séparation entre les deux fils est progressivement augmentée, le mode TEM disparaît et les fils commencent à porter individuellement des modes de Sommerfeld. Le mode TEM porté par le guide d'ondes à deux fils est plus facile à exciter au moyen d'une antenne PC classique que le mode de Sommerfeld dans le guide d'ondes à un seul fil. Dans nos expériences, nous avons démontré la propagation d'impulsions THz à cycle unique sur une bande de 2 THz dans le guide d'ondes à deux fils. Le guide d'ondes s'est révélé être capable de transmettre la totalité du spectre généré par l'antenne PC. Cela démontre la capacité du guide d'ondes à deux fils étudié de transmettre sur une large bande.

Le guide d'ondes à deux fils permet un accès facile à la région de guidage. Cette caractéristique a permis l'insertion d'un réseau de Bragg en polymère entre les deux fils dans le but d'effectuer un filtrage en fréquence. Grâce à l'effet de ralentissement de la lumière causé par le réseau, nous avons observé une amplification de la raie de l'eau à 0.557 THz, qui se trouve dans la région de la bande du réseau.

Dans ce mémoire, un émetteur THz à deux fils a également été démontré. Un morceau de GaAs inséré entre les deux fils du guide d'ondes a servi d'émetteur THz. Suite à l'application

d'une tension électrique sur les deux fils et à la focalisation du faisceau laser pompe sur la pièce de GaA, le dispositif a agi comme une antenne PC. Le signal THz ainsi générée s'est couplé facilement dans le guide d'ondes à deux fils. En utilisant cet émetteur, nous avons observé un signal THz dans le guide d'ondes dont le champ électrique crête est supérieur à celui du guide d'ondes à deux fils couplé à l'antenne PC externe. Cette expérience montre que notre guide d'ondes à deux fils peut être utilisé également comme une source THz. Une telle source peut transporter un champ THz plus fort par rapport au guide d'ondes couplé à une source externe.

Parmi les nombreux sujets d'étude qui pourraient faire suite au travail décrit dans ce mémoire, mentionnons par exemple l'amélioration de la manipulation du guide d'ondes à deux fils en le recouvrant avec une matrice en polymère ayant des propriétés de faibles dispersion et absorption. De plus, de nouvelles façons de traiter les signaux THz au moyen de ce guide d'ondes pourraient être étudiées. Par exemple, des méta-matériaux et de nouvelles conceptions de réseaux de Bragg pourraient être couplés au guide d'ondes à deux fils pour moduler le signal THz. Des améliorations de la THz-TDS pourraient également être envisagées pour l'avenir. Par ailleurs, une analyse théorique en profondeur de l'émetteur THz étudié dans ce mémoire pourrait aider à optimiser ce dispositif. Au total, en combinant des composants de traitement de signal et l'émetteur THz, une nouvelle source THz pourrait être réalisée où il serait possible d'obtenir une impulsion THz ayant la forme temporelle et le spectre désirés.

12. Références

[1] S. Verghese, K. A. McIntosh, and E. R. Brown, "Highly tunable fiber-coupled photomixers with coherent terahertz output power," *IEEE Transactions on Microwave Theory and Techniques,* vol. 45, pp. 1301-1309, 1997.

[2] G. Kozlov and A. Volkov, *Millimeter and Submillimeter Wave Spectroscopy of Solids.* Berlin: Springer-Verlag, 1998.

[3] G. W. Chantry, *Long-wave Optics* vol. 2. London: Academic Press, Inc., 1984.

[4] R. Kohler, A. Tredicucci, F. Beltram, H. E. Beere, E. H. Linfield, A. G. Davies, *et al.*, "Terahertz semiconductor-heterostructure laser," *Nature,* vol. 417, pp. 156-159, 2002.

[5] Y.-S. Lee, *Principles of Terahertz Science and Technology.* New York: Springer, 2009.

[6] P. R. Smith, D. H. Auston, and M. C. Nuss, "Subpicosecond photoconducting dipole antennas," *IEEE Journal of Quantum Electronics,* vol. 24, pp. 255-260, 1988.

[7] A. Nahata, A. S. Weling, and T. F. Heinz, "A wideband coherent terahertz spectroscopy system using optical rectification and electro-optic sampling," *Applied Physics Letters,* vol. 69, pp. 2321-2323, 1996.

[8] H. Hamster, A. Sullivan, S. Gordon, W. White, and R. W. Falcone, "Subpicosecond, electromagnetic pulses from intense laser-plasma interaction," *Physical Review Letters,* vol. 71, pp. 2725-2728, 1993.

[9] D. Banerjee, W. von Spiegel, M. D. Thomson, S. Schabel, and H. G. Roskos, "Diagnosing water content in paper by terahertz radiation," *Optics Express,* vol. 16, pp. 9060-9066, 2008.

[10] M. Naftaly, J. F. Molloy, G. V. Lanskii, K. A. Kokh, and Y. M. Andreev, "Terahertz time-domain spectroscopy for textile identification," *Applied Optics,* vol. 52, pp. 4433-4437, 2013.

[11] L. Yunfei, T. Jiajin, J. Ling, S. Shengcai, J. Biaobing, and M. Jinlong, "Study on terahertz time domain spectroscopy of pine wood nematode disease," *International Conference on Microwave Technology and Computational Electromagnetics ICMTCE*, pp. 271-275, 2009.

[12] http://www.sp.phy.cam.ac.uk/SPWeb/research/thzcamera/WhatIsTHzImaging.htm.

[13] G.-J. K. a. S.-G. J. Yun-Sik Jin, "Terahertz dielectric properties of polymers," *Journal of Korean Physical Society,* vol. 49, pp. 513-517, 2006.

[14] R. M. Woodward, B. E. Cole, V. P. Wallace, R. J. Pye, D. D. Arnone, E. H. Linfield, *et al.*, "Terahertz pulse imaging in reflection geometry of human skin cancer and skin tissue," *Physics in Medicine and Biology,* vol. 47, p. 3853, 2002.

[15] T. G. Phillips and J. Keene, "Submillimeter astronomy [heterodyne spectroscopy]," *Proceedings of the IEEE,* vol. 80, pp. 1662-1678, 1992.

[16] C. A. Schmuttenmaer, "Exploring dynamics in the far-infrared with terahertz spectroscopy," *Chemical Reviews,* vol. 104, pp. 1759-1780, 2004.

[17] M. R. Leahy-Hoppa, M. J. Fitch, X. Zheng, L. M. Hayden, and R. Osiander, "Wideband terahertz spectroscopy of explosives," *Chemical Physics Letters,* vol. 434, pp. 227-230, 2007.

[18] W. Withayachumnankul and D. Abbott, "Metamaterials in the terahertz regime," *IEEE Photonics Journal,* vol. 1, pp. 99-118, 2009.

[19] P. A. Krug, J. Chow, B. J. Eggleton, P. Hill, M. Ibsen, F. Ouellette, *et al.*, "Applications for fiber Bragg gratings in communications," in *Optical Fiber Communications(OFC '96)*, p. 116, 1996.

[20] R. Mendis and D. Grischkowsky, "THz interconnect with low-loss and low-group velocity dispersion," *IEEE Microwave and Wireless Components Letters,* vol. 11, pp. 444-446, 2001.

[21] R. Mendis and D. Grischkowsky, "Undistorted guided-wave propagation of subpicosecond terahertz pulses," *Optics Letters,* vol. 26, pp. 846-848, 2001.

[22] G. Gallot, S. P. Jamison, R. W. McGowan, and D. Grischkowsky, "Terahertz waveguides," *Journal of Optical Society of America. B,* vol. 17, pp. 851-863, 2000.

[23] R. W. McGowan, G. Gallot, and D. Grischkowsky, "Propagation of ultrawideband short pulses of terahertz radiation through submillimeter-diameter circular waveguides," *Optics Letters,* vol. 24, pp. 1431-1433, 1999.

[24] J. Tae-In and D. Grischkowsky, "Direct optoelectronic generation and detection of sub-ps-electrical pulses on sub-mm-coaxial transmission lines," *Applied Physics Letters,* vol. 85, pp. 6092-6094, 2004.

[25] K. Wang and D. M. Mittleman, "Metal wires for terahertz wave guiding," *Nature,* vol. 432, pp. 376-379, 2004.

[26] T.-I. Jeon, J. Zhang, and D. Grischkowsky, "THz Sommerfeld wave propagation on a single metal wire," *Applied Physics Letters,* vol. 86, pp. 161904/1-161904/3, 2005.

[27] P. Tannouri, M. Peccianti, P. L. Lavertu, F. Vidal, and R. Morandotti, "Quasi-TEM mode propagation in twin-wire THz waveguides (Invited Paper)," *Chinese Optics Letters,* vol. 9, pp. 110013/1-110013/4, 2011.

[28] M. K. Mridha, A. Mazhorova, M. Daneau, M. Clerici, M. Peccianti, P.-L. Lavertu, *et al.*, "Low dispersion propagation of broadband THz pulses in a two-wire waveguide," *Optical Society of America Conferences, CLEO*, p. CTh1K.6, 2013.

[29] R. Mendis and D. Grischkowsky, "Plastic ribbon THz waveguides," *Journal of Applied Physics,* vol. 88, pp. 4449-4451, 2000.

[30] S. P. Jamison, R. W. McGowan, and D. Grischkowsky, "Single-mode waveguide propagation and reshaping of sub-ps terahertz pulses in sapphire fibers," *Applied Physics Letters,* vol. 76, pp. 1987-1989, 2000.

[31] H. Han, H. Park, M. Cho, and J. Kim, "Terahertz pulse propagation in a plastic photonic crystal fiber," *Applied Physics Letters,* vol. 80, pp. 2634-2636, 2002.

[32] L.-J. Chen, H.-W. Chen, T.-F. Kao, J.-Y. Lu, and C.-K. Sun, "Low-loss subwavelength plastic fiber for terahertz waveguiding," *Optics Letters,* vol. 31, pp. 308-310, 2006.

[33] M. Rozé, B. Ung, A. Mazhorova, M. Walther, and M. Skorobogatiy, "Suspended core subwavelength fibers: towards practical designs for low-loss terahertz guidance," *Optics Express,* vol. 19, pp. 9127-9138, 2011.

[34] J. Harrington, R. George, P. Pedersen, and E. Mueller, "Hollow polycarbonate waveguides with inner Cu coatings for delivery of terahertz radiation," *Optics Express,* vol. 12, pp. 5263-5268, 2004.

[35] B. Bowden, J. A. Harrington, and O. Mitrofanov, "Low-loss modes in hollow metallic terahertz waveguides with dielectric coatings," *Applied Physics Letters,* vol. 93, pp. 181104/1-181104/3, 2008.

[36] M. Mbonye, R. Mendis, and D. M. Mittleman, "A terahertz two-wire waveguide with low bending loss," *Applied Physics Letters,* vol. 95, pp. 233506/1-233506/3, 2009.

Contents

List of Figures

List of Abbreviations

THz	Terahertz
THz-TDS	Terahertz-Time Domain Spectroscopy
GaAs	Gallium Arsenide
LT-GaAs	Low temperature GaAs
FEL	Free Electron Laser
NDT	Non Destructive Testing
RDX	Research Department Explosive
TNT	Trinitrotoluene
PPWG	Parallel Plate Waveguide
QWP	Quarter Wave Plate
ZnTe	Zinc Telluride
PM	Parabolic Mirror
GVD	Group Velocity Dispersion
PC	Photoconductive
PML	Perfectly Matched Layer
FDTD	Finite Difference Time Domain

Introduction

Overview

Terahertz (THz) radiation comprises the frequency range of 0.1-10 THz in the electromagnetic spectrum (see Fig. 0.1). It lies in between the electrical domain of microwaves and the optical domain of far infrared radiation. At 1 THz, it has a wavelength of 300 μm, a wave number of 33 cm^{-1} and photon energy of 4.1 meV.

This range of frequency was also known as the THz gap due to the lack of availability of well-developed sources and detectors. Thanks to the rapid growth and development in the field of ultrafast optics and semiconductor physics, this THz gap is filling up. Several kinds of detectors and sources have been either developed or improved over the last two decades, such as: photoconductive (PC) antenna [1], electro-optical crystals [2], quantum cascade lasers [3], etc. Terahertz radiation, due to its several unique properties, caught the immediate attention of the research community. This radiation can easily pass through dielectric materials such as paper [4], cloth [5], wood [6] and plastics [7] unlike the infrared radiations which is absorbed by these materials. THz radiation is also shorter in wavelength than microwave radiations, which makes it a very good candidate to image macroscopic dielectric structures with sub-millimeter level or even higher resolution. Given its low energy (4.1 meV at 1 THz), THz is non-ionizing in nature and does not represent any health hazards for living tissues, unlike, e.g., X-rays. Although THz radiation is absorbed by water, it can still be used for bio-medical imaging of tissues [8], based on their water content information. Also, this radiation is emitted by extra-terrestrial objects as a

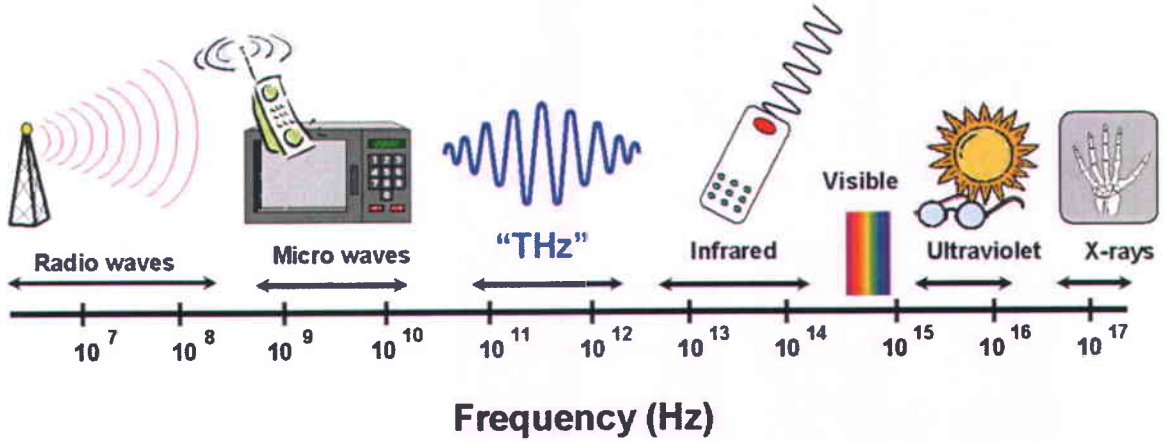

Fig. 0.1 Electromagnetic spectrum (Figure source [9])

part of their black-body emission and specific compounds whose rotational and vibrational spectra lie at THz frequencies [10].

Over the past two decades, THz radiation has been extensively studied for applications in Terahertz-Time Domain Spectroscopy (THz-TDS) [11]. This technique is used for material characterization and spectroscopy in the THz region of the electromagnetic spectrum. The particularity of this technique lies in its ability to retrieve the complex refractive index of a material under study. Such a measurement is possible with THz-TDS because the real electric field of the THz radiation is recorded instead of the intensity (as typically measured in optics). Therefore, this technique shows clear advantages in comparison to Fourier Transform Infrared (FTIR) spectroscopy [12], where only the intensity of the radiation can be measured. THz-TDS has helped in the characterization of several polymers such as Polyethylene, Polypropylene, Teflon, Polycarbonate, etc. [13]. It has also been used for the spectroscopy of small bio-molecules (such as amino acids, polypeptides, nucleic acid, etc.) [14], bio-macromolecules (such as DNAs, RNAs, proteins, etc.) [15] and specific explosives such as Trinitrotoluene (TNT) and Research Department Explosives (RDX) [16]. Due to the benefits of THz radiation over microwaves and infrared radiation and due to its non-ionizing nature, this radiation has found large potential for imaging in industrial, bio-medical and security application [17]. In the industry, THz is employed for inspection of packaged goods, quality control and process monitoring [18]. In the bio-medical field, THz radiation has been investigated for imaging in medical diagnostics (such as effective detection of epithelial cancer [8]), 3D imaging of dental tissue [19], etc. Security applications include development of THz systems for remote detection of concealed weapons and inspection of packaged goods to detect explosives. The advancement in THz technology also boosts developments in fundamental physics. Indeed several phenomena, such as intraband transition in semiconductors [20] and correlated electron systems [21] require enhanced THz technology. A field of application where development in THz technology can make significant amount of contribution is communication [22]. Microwave radiation has been serving the area of wireless communication over the past century and is still growing [23]. However, the increasing demand for mobile communication bandwidth (several tens of Gbit/s) will eventually saturate the communication capabilities of the currently regulated electromagnetic spectrum (<300 GHz) [24]. A possible solution could be relying on THz radiation since higher bandwidth can be achieved by switching to a higher frequency region.

Motivation and objectives

With increasing population, industries, business organisations and infrastructure, the demand for higher rates of data transfer over long distances (fiber optics network) and short distances (wireless network) is increasing day by day. In order to achieve higher data transfer rates in short distance communication, the bandwidth of the current microwave based communication system needs to be increased. By moving to the THz spectral region, which is higher in frequency than microwaves, the issue of achieving higher bandwidth can be addressed.

To realize a THz communication network, basic building blocks for a communication system needs to be developed for THz frequencies. These include, sources, detectors, waveguides and signal processing components like Bragg gratings [25]. Among these components, waveguides will play an essential role by transferring THz signal over long distances with minimal losses when compared to free space propagation of THz, which is limited by diffraction and water absorption. Furthermore, the development of THz waveguides will also be useful for enhancing THz-TDS. Both these fields however, will need low-dispersion, broadband waveguides. In addition, accomplishing THz signal processing directly in waveguides will be an added advantage for the future THz networks as it will avoid the use of intermediate components that can introduce additional losses.

The objective of this thesis is to develop a waveguide for long distance THz signal propagation and to lay the basis for guided- wave signal processing. We have selected a two-wire metallic waveguide scheme as the main target of our investigation due to its expected very low-dispersion and minimal bending losses. The low dispersion associated with a relatively tight confinement between the wires, opens up new prospects for THz signal processing, enhanced THz-TDS and nonlinear studies. In this thesis we exploit these guiding characteristics for THz signal processing by inserting a polymer grating in between the wires. We then demonstrate the possibility of realizing an active waveguide, with the THz pulse generated directly inside the guiding structure. This is achieved by optically pumping a Gallium Arsenide (GaAs) semiconductor component inserted in between the two wires of the waveguide and applying a proper bias voltage to the waveguide.

Scope of the thesis

In this thesis we describe the characterisation of a two-wire waveguide for THz radiation. We shall show that the waveguide supports the propagation of broadband THz radiation (> 2 THz) over a 20 cm distance with low dispersion (so that the single-cycle pulses can be transmitted without distortions). We shall also experimentally demonstrate a signal processing application (namely, spectral filtering) in the two-wire waveguide, by means of a polymer grating.
The thesis is divided into five chapters.

In chapter 1 we give an introduction to the field of THz in general. We briefly describe some of the sources and detectors for THz radiation and the various sectors where THz technology has been used or can be potentially employed. We then discuss the motivations that push us to develop low dispersion and broadband THz waveguides (two-wire waveguides) and present a literature review on THz waveguides.

In chapter 2 we first provide an introduction to the theory of the two-wire waveguide. We then describe the two-wire waveguide developed and characterized in this thesis. We describe the challenges and the used experimental setup. Finally, we discuss the results we obtained.

In chapter 3 we shall describe an experiment on signal processing (spectral filtering) in a two-wire waveguide with the use of a polymer grating. The chapter starts with a brief discussion on the theory of fiber Bragg gratings, followed by an account of previous works on periodic structures for THz radiation. We then describe the results obtained by using a polymer structure as a grating inside the two-wire waveguide and discuss the experimental results obtained. We conclude the chapter by describing the enhancement of one of the water lines of the THz spectrum. This enhancement is obtained by virtue of the slow-light effect.

In chapter 4 we discuss the possibility of generating THz radiation inside the waveguide by inserting a thin piece of GaAs in between the two wires. The semiconductor acts as a source of THz radiation once a bias voltage is applied on the waveguide wires. The emitted THz radiation is automatically coupled into the two-wire waveguide.

In chapter 5 we draw the conclusions and discuss the future perspectives of this work.

Chapter 1: Literature review

1.1 Terahertz generation and detection

The investigation on THz radiation long suffered from the lack of sources and detectors suitable for this spectral region (the so-called THz gap). The developments in semiconductor technology and ultrafast optics over the last two decades helped in filling this gap. During this period, sources and detectors based on photomixers [26], photoconductive (PC) antennas [27], electro-optic crystals [2], backward wave oscillator (BWO) [28], thermal detectors [29], etc. were developed. They can be broadly classified under two categories: (i) continuous wave (CW) THz based sources and detectors and (ii) pulsed THz based sources and detectors. Continuous wave sources for example include: photomixers, nonlinear crystals (2^{nd} order nonlinearity) [30, 31], quantum cascade lasers [3], etc. Thermal detectors and heterodyne based detection systems are commonly used as CW THz detectors. Some of these CW sources, for instance, can be used for THz wave imaging (see reference [32, 33]). Photoconductive antennas and electro-optic crystals (such as Zinc Telluride, ZnTe) are being widely employed for THz-TDS [11] because of their ability to emit and detect broadband THz pulses. In this thesis, a THz source based on a PC antenna and a detector based on ZnTe crystal have been used for broadband characterization of our two-wire waveguide. A typical THz single cycle pulse generated by a PC antenna and detected by an electro-optical sampling technique is shown in Fig. 1.1 (signal generated and detected during the experiments concerning the development of our work).

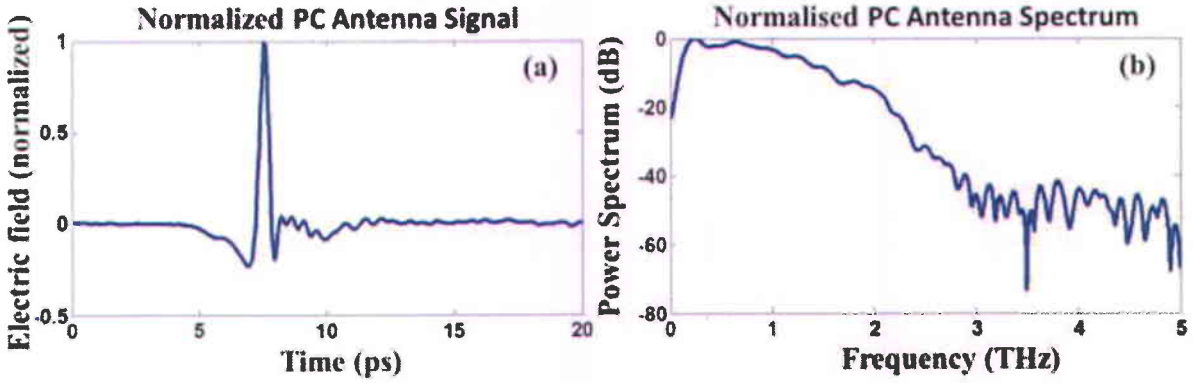

.Fig. 1.1 (a) THz signal and (b) its corresponding spectrum generated by a PC antenna and detected via electro-optical sampling. All the curves are normalized.

In the following subsections we provide a brief description of various sources and detectors for THz radiation

1.1.1 CW sources and detectors

a) Photomixing :

In photomixing, also known as optical heterodyne down conversion, two lasers with different frequencies (ω_1 and ω_2) interact to form electromagnetic radiation with lower frequencies ($\omega_{beat} = \omega_1 - \omega_2$), i.e. in the THz range in our case. The device is basically a PC switch consisting of a semiconductor substrate with an antenna deposited on it (typically a logarithmic spiral [26]). The incident laser beams generate charge carriers in the PC switch. On application of voltage on the electrodes, the induced photocurrent oscillates at the beat frequency (ω_{beat}) of the two incident laser beams. The oscillating photocurrent thus creates CW THz pulses at the beat frequency. Hence, the desired THz frequency can be generated via the photomixing method by tuning the beat frequency. In general, a low temperature grown GaAs substrate serves as a suitable material for THz generation using this technique. This is due to the high mobility and short life time of the charge carriers that are generated in this process. Such sources generate THz output power in the microwatts range, which is lower than other CW THz sources.

b) Far-infrared gas lasers:

Molecular gases such as CH_3F, CH_3OH, NH_3 and CH_2F_2 can serve as a gain medium to realize THz lasers with properly implemented technology. These molecules have permanent dipole moments, and their rotational transitions lie in the THz region. For example CH_3OH has laser lines at 0.245, 0.525, 2.52, 4.25, 4.68, 7.1 and 8.0 THz with a recorded output power of nearly 10, 40, 100, 100, 20, 10 and 10 mW, respectively [34].

c) P-type germanium lasers:

The p-type germanium lasers are basically electrically pumped, all-solid-state lasers. A germanium crystal, generally doped with beryllium, acts as the active medium where lasing occurs in the presence of crossed electric and magnetic fields. In the presence of a magnetic field, the holes in the active medium act as charged particles that undergo circular motion at cyclotron frequencies. The spatial confinement of the active medium creates discrete energy

levels for the holes, which are also known as Landau levels. Application of the electric field excites the holes from lower to higher Landau levels. Terahertz radiation is thereby generated due to stimulated transitions between two of such levels. For the operation of such laser, the active medium needs to be maintained at low temperatures (< 40 K). An in depth study on the working of such lasers is provided in reference [29]. The THz radiation typically generated has a pulse energy of few micro-joules and pulse duration of several microseconds. The average output power reaches up to a few watts, and the frequency can be tuned from 1 to 4 THz by changing the electric and magnetic field strengths [35].

d) Schottky diode frequency multipliers:

A Schottky diode based frequency multiplier in electronics is analogous to a nonlinear crystal which can produce harmonics of optical waves. Schottky diode based sources can therefore emit THz radiation by generating harmonics of the incoming microwave frequencies. For example, a frequency tripler based on microwave technology can generate CW THz sources with 22-25 mW output power in the 0.552 to 0.645 THz range [36].

e) Quantum cascade lasers:

Quantum cascade lasers (QCL) are based on semiconductor heterostructures, which consist of periodically alternating layers of dissimilar semiconductors (superlattice structure). Owing to the 2D quantum confinement of the layers, such heterostructures form discrete energy levels (also called subbands) at different layers. Following the application of an external bias, the induced inter subband transition of an electron in one period leads to the emission of electromagnetic radiations in the THz region. The same electron undergoing the transition tunnels to the adjacent period where it undergoes a second inter subband transition. This process continues until the electron reaches the end of the superlattice. This phenomenon of electron tunneling in the subsequent periods is known as cascading. Due to the cascading process, a single electron can generate several THz photons. In literature, one of the first optimized THz QCL based on chirped superlattice was reported in 2002 [3]. Presently, a commercial QCL capable of producing a peak power level > 20 mW and an average power levels > 1 mW at frequencies between 1.8 and 5 THz is available in the market [37]. However, to get the maximum power, these QCL based THz sources need to be maintained near liquid He temperature, i.e. 4 Kelvin.

f) Backward wave oscillator:

Backward wave oscillators (BWO) are vacuum tubes based systems and are also known as carcinotrons. Here, THz radiation is generated from the interaction between an electron beam and a periodic structure placed inside the BWO (see reference [28] for detailed description). The electron beam gains kinetic energy from the voltage bias applied in the BWO and this kinetic energy is eventually transformed into THz radiation. Hence, the frequency of the THz radiation emitted can be tuned by changing the bias voltage on the BWO. The BWO described in reference [28] can operate from 0.03 to 1 THz. The output power ranges reaches up to 100 mW below 200 GHz and falls down to 1mW at 1 THz.

g) Free electron lasers:

Free electron lasers (FEL) are based on the relativistic motion of electron beams. The electron beam generated from a particle accelerator and moving close to the speed of light, is sent through a series of magnets. These magnets are arranged in such a way that the periodic, transverse magnetic field induces a sinusoidal oscillation of the electrons, which in turn generates monochromatic radiation (for more details see reference [29]). Such THz FEL systems are very large, bulky and occupy a lot of space. Only a few of them are available around the world. For instance, the THz FEL facility, named FIREFLY, which is available at Stanford CA (USA), generates THz radiation in the range 4 to 20 THz and another facility, named CLIO, which is located at LCP in Orsay (France) generates THz radiation in the range 2 to 100 THz [29].

h) Thermal detectors:

Thermal detectors are generally equipped with a radiation absorber attached to a heat sink. The radiation energy absorbed is converted into heat. A thermometer then measures the temperature increase. In such devices, the absorber has a very low heat capacity in order to display very small changes in temperature. To determine the absorbed radiation energy, the detector has to be calibrated as a function of the increase in temperature. Based on different type of schemes to measure the change in temperature, different kinds of thermal detectors are available. These include bolometers, pyroelectric detectors and Golay cells. A bolometer employs a material whose electrical resistance is sensitive to temperature. For high detection sensitivity, bolometers are operated below liquid helium temperature. In a pyroelectric detector, the change in spontaneous electric polarization of a pyroelectric material due to change in temperature is measured for detecting THz radiation. Golay cells consist of an absorbing film which transfers

the thermal energy of the radiations to an attached gas chamber. The expansion of the gas is measured by an optical setup to determine the rise in temperature and thereby detecting the incident radiation power. (For more details see reference [29]).

i) Heterodyne detectors:

Heterodyne detection is based on frequency down conversion in a nonlinear device. In analogy to photomixing, the incident THz radiation is mixed with a reference radiation (also known as local oscillator) at a fixed frequency. While gas lasers are generally used as local oscillators to detect radiations greater than 1 THz, solid-state emitters such as QCLs are considered as promising local oscillators in the region 0.1 to 1 THz. Some of the most sensitive mixers for THz detection are cryogenic detectors (hot electron bolometers) based on indium antimonide (InSb) [38] or niobium (Nb) and niobium nitride (NbN) in a superconductor phase [39, 40].

1.1.2 Broadband pulsed sources

a) Terahertz generation in air:

Terahertz radiation can be generated in air by creating an air plasma [41]. The air plasma is created by focusing high power laser pulses, strong enough to produce optical field ionization. The subsequent generation of THz radiation involves oscillations of electrons through the ponderomotive force. The strength of the THz signal generated in this process can be further enhanced by using a strong bias field [42] or by focusing the second harmonic of the pump laser used in the interaction region [43]. With the method of THz generation by second harmonic enhanced air plasma, a field amplitude greater than 100 kV/cm has been achieved with 20 mJ optical pulses [44]. Recently, a THz electric field strength of 4.4 MV/cm, the highest ever measured, has been reported in reference [45]. The technique of THz generation by gas ionization, however, requires the implementation of high power regenerative amplifiers, which makes it quite expensive to employ.

b) Terahertz generation and detection by photoconductive antennas:

A PC antenna can be used both as a source and as a detector (see Fig. 1.2, for a schematic diagram). It consists of two metallic electrodes deposited on the surface of a semiconductor substrate. The opposite side of the antenna may be featured with a hyper-hemispherical lens in order to collimate the emitted THz radiation or to focus the incident THz beam for detection. The

pump beam (with central frequency depending on the employed semiconductor) is focused between the two electrodes. As the energy carried by the photons of the incident laser beam is greater than the band gap of the substrate, the laser excites the electrons from the valence band to the conduction band. When a voltage bias is applied to the electrodes during excitation by the laser, the induced electric field drives the excited electrons into generating a transient current. This time varying current radiates THz pulses, following the laws of classical electrodynamics. The THz electric field is given by the simple equation:

$$E_{THz} = \frac{1}{4\pi\varepsilon_0}\frac{A}{c^2 Z}\frac{\partial J(t)}{\partial t} = \frac{A}{4\pi\varepsilon_0 c^2 Z}\frac{\partial N(t)}{\partial t}\mu E_b \tag{1.1}$$

where

$$J(t) = N(t)e\mu E_b \tag{1.2}$$

is the time dependent current density. In these equations, A is the area in the gap illuminated by the laser light; ε_0 is the vacuum permittivity; c is the speed of light in vacuum; Z is the distance between the field point and the THz source; N is the density of the photo carriers (which depends on the laser pulse shape and carrier lifetime of the semiconductor substrate); e is the electronic charge; μ is the electron mobility, and E_b denotes the electric field bias. A detailed study on the effect of the pump power and bias voltage on the THz field emitted by different kinds of PC antennas is available in reference [46]. For example, reference [46] reports the generation of THz radiation with a power of 0.6 μW from a strip line PC antenna that was biased with 100 volts and excited by a 15 mW pump laser. By increasing the power of the pump beam or by increasing the voltage bias, the strength of the THz field generated by a PC antenna can be increased. However, in the case of PC antennas on a semi-insulating GaAs substrate, the power of the emitted THz radiation saturates with the increase in power of the pump beam [46] due to screening of the bias field by the induced photocarriers. Also a PC antenna cannot be biased beyond the breakdown voltage of the substrate. For example, a low-temperature grown GaAs (LT-GaAs) has a breakdown voltage of 500 kV/cm [46]. Hence, in order to prevent a PC antenna grown on LT-GaAs with a gap size of 100 μm from getting damaged, it should not be biased beyond 5 kV.

In the case of PC antenna based detectors, the incident THz beam drives the photo-excited electrons towards one of the electrodes for appropriate polarization direction of the THz electric

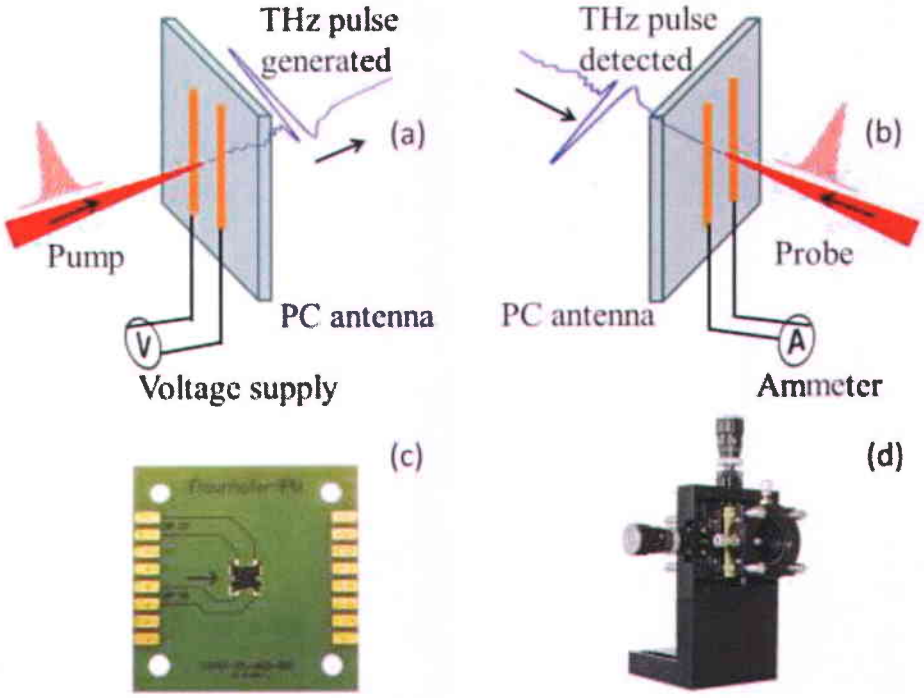

Fig. 1.2 (a) Terahertz PC (photoconductive) antenna as a source and (b) as a detector with arrows indicating the direction of propagation. (c) A commercially available PC antenna (Tera-8 from Menlo Systems) and (d) its mount.

field. By measuring the current thus created, the relative value of the THz electric field can be retrieved.

c) Terahertz generation and detection by an electro-optic crystal:

An electro-optic crystal without inversion symmetry, i.e. having second order electric susceptibility, $\chi^{(2)}$, could be used for the generation and detection of THz radiation. The generation of THz radiation from a $\chi^{(2)}$ crystal is based on the principle of optical rectification, also called difference frequency generation (DFG) in nonlinear optics. In $\chi^{(2)}$ crystals, with a high incident laser field, the polarization (P) varies nonlinearly with the electric field and is generally not collinear to the electric field as can be seen from the Taylor's series expansion:

$$P_i(t) = \sum_j \chi_{ij}^{(1)} E_j(t) + \sum_{j,k} \chi_{ijk}^{(2)} E_j(t) E_k(t) + \sum_{j,k,l} \chi_{ijkl}^{(3)} E_j(t) E_k(t) E_l(t) + \ldots \qquad (1.3)$$

where $\chi_{ij}^{(1)}$ denotes the linear susceptibility tensor, and $\chi_{ijk}^{(2)}$ and $\chi_{ijkl}^{(3)}$ denote the 2nd and 3rd order susceptibility tensors, respectively. Based on the 2nd order non-linear coefficient and phase

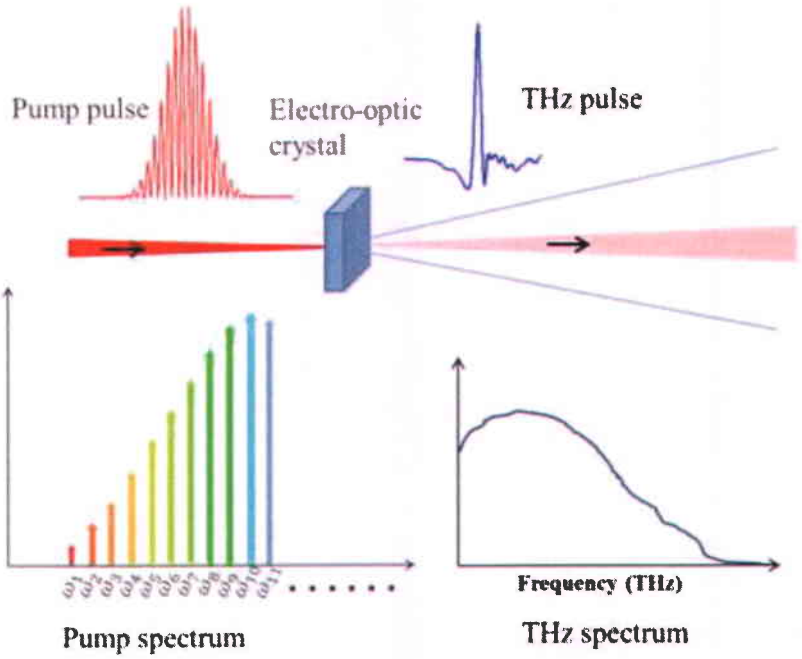

Fig. 1.3 Schematics of THz generation by optical rectification technique. The different frequency components of the mode locked laser beam (ω_1, ω_2, ω_3, ...) undergo DFG to generate a broadband THz spectrum.

matching criteria in a $\chi^{(2)}$ crystal, the frequency components of a mode locked laser beam produce THz radiation, through the mechanism of intra-pulse DFG (see Fig. 1.3 for schematics).

The use of such crystals as detectors for THz radiation is made possible thanks to the linear electro-optic effect, where the refractive index of a medium is linearly proportional to the applied electric field. A scheme for the detection of THz radiation by the electro-optical sampling technique is shown in Fig. 1.4. It consists of a $\chi^{(2)}$ crystal followed by a quarter wave plate, a Wollaston prism and a balanced photodetector. In this system, the incident THz electric field (both magnitude and direction) creates a nearly DC electric field in the crystal as compared to the much shorter probe beam. This nearly DC field induces birefringence in the detection crystal. Without the presence of any DC electric field, the linearly polarized probe beam is transformed into circular polarization (with s and p components of equal intensities) by the quarter wave plate placed after the detection crystal. When the THz radiation and probe beam are coincident in time and space, the probe beam (pulsed laser beam) undergoes further changes in

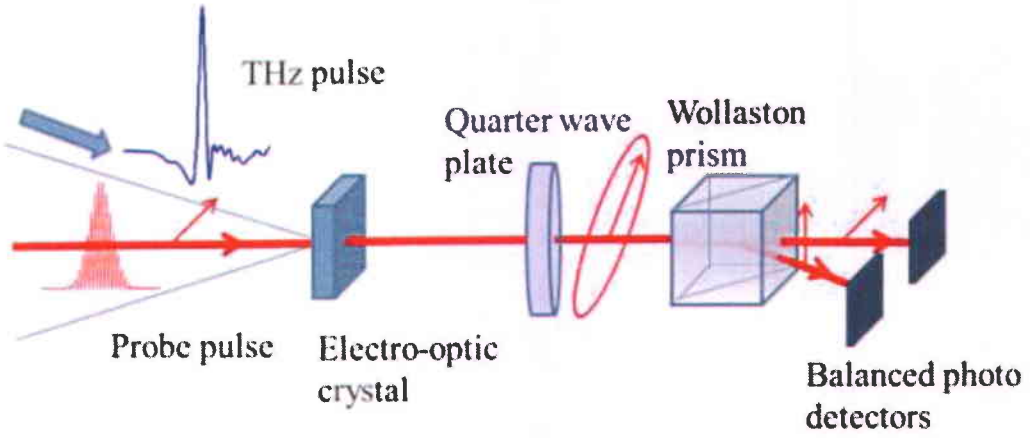

Fig. 1.4 Schematics of detection by electro-optical sampling technique. The THz radiation is focused on the electro-optic crystal where it modulates the polarization of the probe pulse. The arrows indicate the final polarization directions of the probe pulse.

its polarization due to the THz electric field-induced birefringence in the $\chi^{(2)}$ crystal. The birefringence transforms the circularly polarized probe beam into an elliptically polarized beam with unequal s and p polarization components. The difference between the intensities of the s and p components is linearly proportional to the electric field of the THz beam to be detected. Hence, by measuring the difference between the intensities of these two polarized states on a balanced photodetector, the relative THz electric field can be retrieved. For further details on the physical principle underlying the use of $\chi^{(2)}$ crystals as a THz source and detector, see references [29, 47].

1.2 Terahertz applications

With the gradual filling of the THz gap, scientists and engineers identified many opportunities where this region of the electromagnetic spectrum could be used for scientific and industrial applications. THz radiation has found application in the field of spectroscopy and material characterization on the one hand, and imaging with sub-millimeter resolution on the other. Even spectroscopy and imaging combined together can find potential application in material inspection. This section discusses some of the major applications of THz radiation.

a) Non-destructive testing:

Non-destructive testing (NDT) aims at examining objects without compromising their functionality. On the one hand, ultrasound and X-rays have been used in NDT over a long time for material inspection, medical diagnostic and quality control during manufacturing. On the

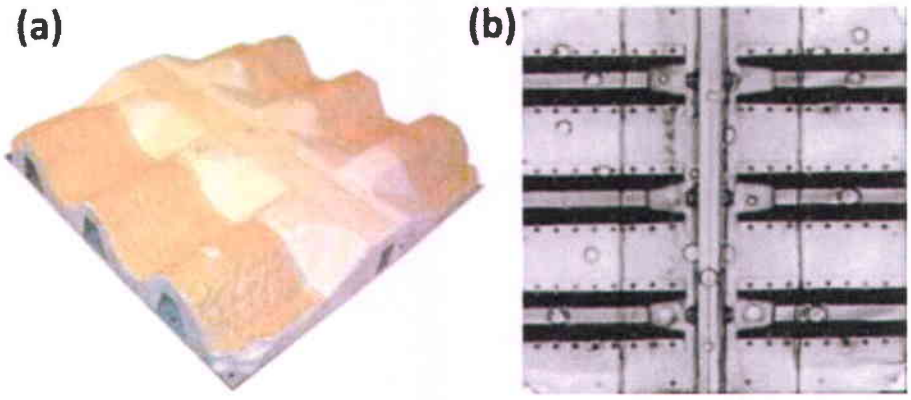

Fig. 1.5 (a) Optical photo of a 2 × 2 panel sample and (b) its THz wave image [47].

other hand in destructive testing, the materials being tested are destroyed, and not suitable for future use. The THz radiation, unlike infrared radiation, is transparent to several dielectric materials such as paper [4], cloth [5], wood [6], polymers [7], etc.. Also, being THz radiation shorter in wavelength than microwaves, can provide sub-millimeter level resolution for imaging, i.e. much lower than microwaves. Due to these properties, THz radiation has been used e.g. for space shuttle foam inspection (see Fig. 1.5), armor plate inspection, rust under paint and carbon fiber composite inspection in either a reflective or transmissive imaging configuration, depending on the material being tested [47].

b) Security check:

Security is a major concern in several countries around the world, pushing the scientific community to develop new technologies for detecting potential threats. Security threat may come from harmful chemicals, biological weapons, explosives and several metallic objects. THz imaging techniques and THz-TDS aim to solve a certain fraction of these security concerns. Due to its unique properties, THz radiation can be employed to detect biological, chemical weapons or explosives such as RDX and TNT [16] (see Fig. 1.6 for their THz absorption spectrum) remotely through optically opaque obstacles such as paper envelopes or clothes.

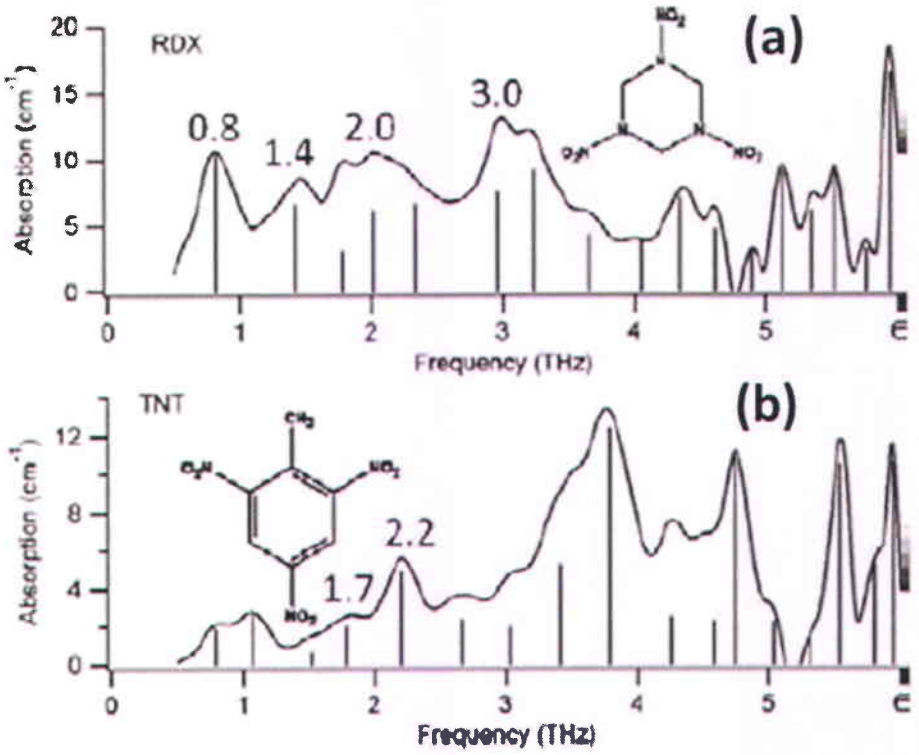

Fig. 1.6 Spectral features of explosives (a) RDX and (b) TNT in 0 to 6 THz range [16].

c) Bio-medical applications:

Many spectral features of several biological molecules and macro-molecules lie in the THz range. Hence, THz radiation has been employed to carry out the spectral analysis of biological molecules like 1-4 glycine molecules [14] and macro-molecules such as DNA, bovine serum albumin and collagen in the 0.1-2 THz range [15]. Terahertz radiation has also been employed for quality control of pharmaceutical products, e.g. to determine the ratio between two different isomers of ranitidine hydrochloride [48] (a popular drug used in treatment of stomach diseases, such as gastric ulcer). THz radiation, due to its low photon energy is also located in an ideal frequency range for examining active biomedical samples under normal conditions without damaging them. In addition, due to the sensitivity of THz radiation to water and bio-molecules, refractive index and absorption coefficient of healthy skin and cancer tissue (basal cell carcinoma) appear to show clear differences in the THz band [49]. Although THz radiation cannot penetrate deep into the human body due to its high water content, THz wave imaging can still be used in the reflection geometry to diagnose skin cancer [8] (see Fig. 1.7).

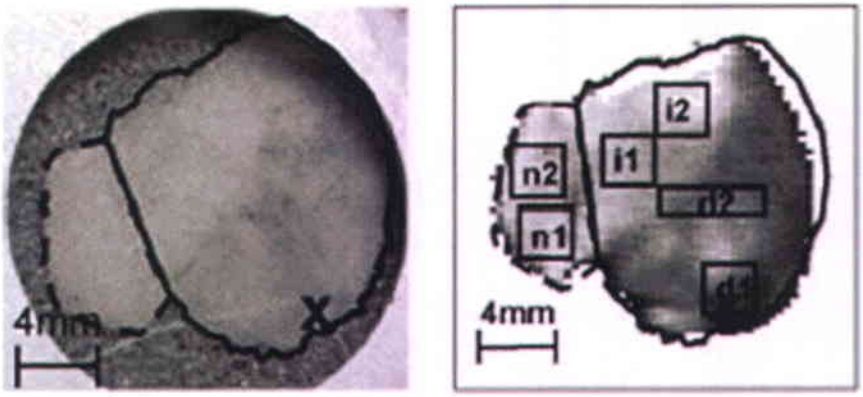

Fig. 1.7 The images of cancerous areas (boundary with solid curves) have been compared with healthy area (boundary with dashed curves) [8].

d) Fundamental science:

Fundamental sciences have witnessed new developments following the advancement in the field of THz technology. Terahertz radiation has now been used to investigate a wide range of phenomena extending from lattice vibrations and intra-band transitions in semiconductors to the dynamics of complex fluids, electron spins, and strongly correlated electrons. More specifically, THz-TDS has been used to: investigate the temporal evolution of Coulomb screening and plasmon scattering in GaAs [20], to probe scattering processes of charged carriers in a photo-excited sapphire crystal [50] and to observe the opening of a superconducting gap in MgB_2 [21]. Some of the phenomena investigated could be used in next generation technologies, like ultrahigh speed and ultra-large capacity information processing.

e) Space applications:

The blackbody radiation spectrum of interstellar objects (dust, light and heavy molecules) with temperatures between 30 Kelvin and 2.7 Kelvin (cosmic background) lies from wavelengths of few μm to the centimeter range [10, 51] (see Fig. 1.8), covering the THz radiation band (around 300 μm). As a result, sub-millimeter detectors can help astronomers to probe into early universe, star forming regions and detect the presence of molecules (such as water, oxygen, carbon monoxide and nitrogen) in outer space. To realize such applications, heterodyne detectors and thermal detectors are needed for lower and upper THz band respectively. For example, the use of high resolution heterodyne receivers has revealed spectroscopic signatures of gases in the earth's upper atmosphere at sub-millimeter wavelengths [52].

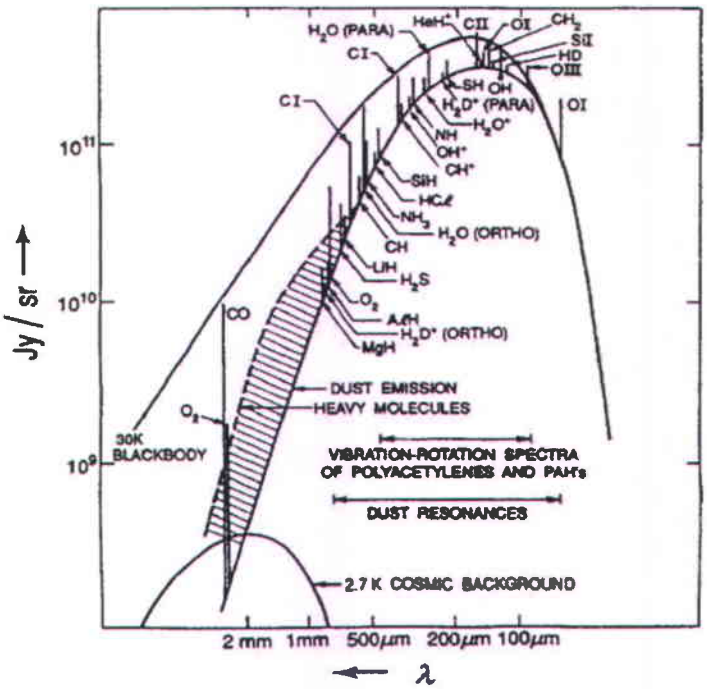

Fig. 1.8 Radiation energy vs wavelength showing the 2.7 Kelvin cosmic background, 30 Kelvin blackbody radiation and molecular emission lines in the sub-millimeter wavelength region [10].

1.3 Literature review on waveguides

Distortion-free propagation of broadband THz pulses over a long distance is a very critical issue, which needs to be addressed. Achieving such a feat can open up new horizons for communication in the THz regime. On one hand, various metallic structures, generally used in the microwaves and radiofrequency regime, have been investigated for THz wave guiding. These structures include parallel plate waveguides (PPWG) [53, 54], rectangular waveguides [55], circular waveguides [56], coaxial cables [57], single wire waveguides [58, 59] and two-wire waveguides [60]. Figure 1.9 gives an overview of the various metallic structures investigated for THz wave guiding. In addition, several dielectric-based waveguides, generally used for optical, far-infrared and infrared radiation, have also been proposed and studied. To name a few structures: dielectric ribbon waveguides [61], sapphire fibers [62], plastic photonic crystal fibers [63], sub-wavelength fibers [64, 65], and many other examples. Several composite structures made of dielectric and metal [66, 67] have also been demonstrated and studied. Figure 1.10 gives an overview of the various dielectric structures used for THz wave guiding along with the materials used.

Type of metallic waveguides	Metals reported to be used
Parallel plates 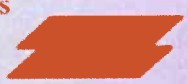	Aluminium and Copper
Rectangular 	Brass plates
Coaxial cable 	Copper with teflon support
Single wire 	Copper and Stainless-steel
Two-wire 	Copper and Stainless-steel
Circular metal tube 	Stainless-steel

Fig. 1.9 Different types of metallic waveguides for THz.

Type of dielectric waveguides	Dielectric materials reported to be used
Ribbon 	Polypropylene
Subwavelength fiber 	Teflon, Sapphire, Polyethylene
Photonic crystal fiber 	Teflon, Topas
Dielectric pipe/ tube structure 	Polypropylene

Fig. 1.10 Different types of dielectric waveguides for THz

1.3.1 Dielectric waveguides

Most of the dielectric materials available are dispersive and induce losses at THz frequencies. For example in reference [61] it is reported that a sub picosecond THz pulse was broadened to over 15 picoseconds with a positive chirp. Similar dispersive effects were numerically and experimentally observed in other dielectric based waveguides too. In order to address the problems of losses and dispersion in dielectric-based waveguides, researchers proposed and tested low loss materials with different geometries. These materials include Teflon [68, 69], polyethylene [64] and polymer based waveguides with sub-wavelength structures [64, 65, 70]. Figures 1.11 (a-b) show typical refractive index and loss profiles as a function of frequency for few commonly used polymers in the THz regime. As can be seen in Fig. 1.11 (b), these polymers tend to have higher losses towards higher frequency regions.

The sub-wavelength dielectric structures were designed to address the problem of losses by confining most of the THz radiation into the air region instead of the dielectric. But such structures suffer from the problem of narrow bandwidth and losses at higher frequencies. With these sub-wavelength waveguides, electromagnetic fields with lower frequencies lie mostly in the air region and hence are attenuated less, whereas higher frequencies stay confined in the dielectric region and thus get dispersed and attenuated. The distortion and attenuation of THz pulses in dielectric waveguides make such waveguides inconvenient for being employed in long distance signal transferring and in THz-TDS. Although composite structures [66, 67] introduce lower losses, they are also dispersive due to presence of higher order modes.

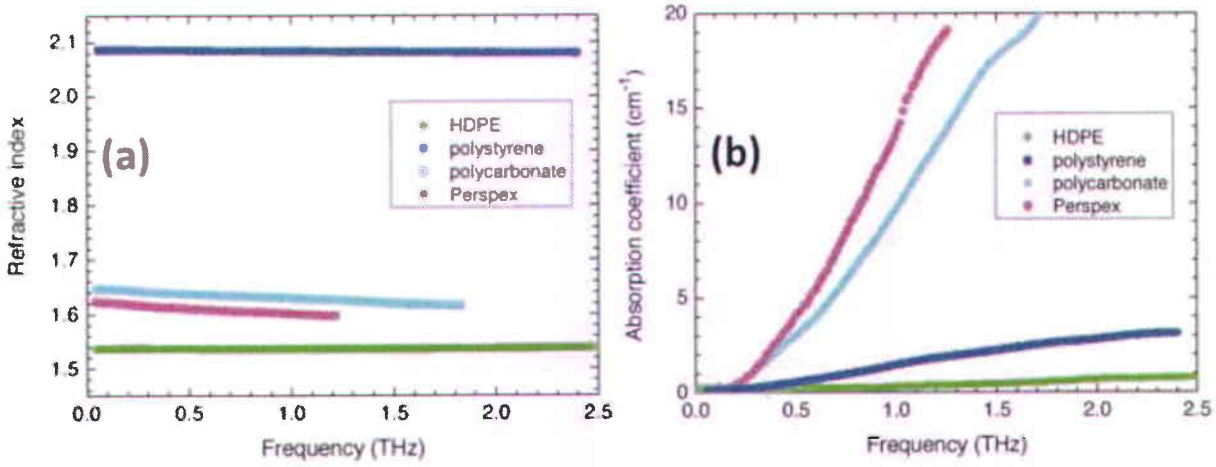

Fig. 1.11 (a) Refractive index profile and (b) absorption spectrum of some commonly used Polymers in the THz region (figure source [13]).

1.3.2 Metallic waveguides

Metallic waveguides, as compared to dielectric waveguides, have shown very low dispersive propagation in the THz regime. These waveguides support a transverse electromagnetic mode (TEM) which is comparable to a free space propagating mode where all frequencies travel with the same speed. Experimentally, PPWGs [53, 54], single wire waveguides [58, 59] and two-wire waveguides [71] have been demonstrated to support the propagation of THz radiation with low dispersion over 2 THz [53], less than 0.6 THz [58] and less than 0.5 THz [71] of bandwidth, respectively. Single wire waveguides modes (Sommerfeld modes), however, are very difficult to excite by the generally available THz sources (which are linearly polarized). Hence, there is no efficient mode matching between the source and the radially polarized mode of a single wire. Thus, custom designed sources become necessary [59]. Metallic PPWG have shown excellent characteristics in transferring THz radiation without distortion and have been successfully utilized to extract fine spectral features of compounds like RDX and TNT. These compounds are critical to be recognized for enabling homeland security [72]. However, two dimensional confinements is not possible in PPWG due to beam spreading in the unguided dimension [53], thus limiting the use of PPWG over long propagation lengths.

As will be shown in this thesis, two-dimensional confinement accompanied by low dispersion propagation can be achieved via a metallic two-wire waveguide [60, 71]. In this work the two-wire waveguide investigated in [71] in the sub-GHz range, has been improved a step further. Specifically, we experimentally demonstrated that two wire waveguides can carry sub-picosecond THz pulses over 2 THz with low dispersion over a distance of 20 cm [73]. The next chapter will illustrate the salient features of the developed two-wire waveguide and also discuss the experimental results obtained.

1.4 Conclusion

In chapter 1, we reviewed various continuous wave and pulsed THz based sources and detectors. We also enlisted some applications of THz radiation in the fields of imaging, material characterization, THz-TDS, security, astronomy, etc. We then reviewed various dielectric and metallic waveguides for THz radiation reported in the literature. The use of dielectric waveguides for long distance THz guiding is limited by THz absorption and dispersion in the dielectric medium. Special metallic waveguides such as single-wire waveguides, PPWG and

two-wire waveguides can carry THz pulses with low-dispersion. Among these three typologies, two-wire waveguides possess the unique characteristics of enabling both linear polarization and two-dimensional mode confinement, unlike the single wire waveguide and the PPWG. Linear polarization allows more efficient coupling with the input wave, and two-dimensional confinement avoids unwanted losses due to diffraction, in the unguided dimension. Hence, the study of the THz two-wire waveguide for broadband THz propagation becomes essential and is therefore the main focus of this thesis.

Chapter 2: Terahertz two-wire waveguide

2.1 Theory of the two-wire waveguide

The two-wire waveguide has been theoretically studied for THz wave guiding [60, 74] and experimentally reported for the GHz region [71]. A basic scheme of a two-wire waveguide is shown in Fig. 2.1. The two-wire mode lies in the **x-y** plane and it propagates in the **z** direction. A two-wire waveguide carries a low-dispersive TEM mode when the wire separation S is close to the wavelength of operation [60]. The low-dispersive characteristics associated with relatively high confinement, achievable in the two-wire waveguide, increases the prospects for nonlinear studies in such waveguides.

Theoretical studies on the two-wire waveguide [60, 74] showed the behavior of the guided TEM mode as the two wires are separated. The simulated mode distribution in the two-wire waveguide for different wire separations at 1 THz frequency (300 μm wavelength) for wires radius of 125 μm is shown in Fig. 2.2. These mode simulations were carried out by using a commercial Eigenmode mode solver from Lumerical. Three different simulations were carried out for the three different wire separations of 300 μm, 500 μm and 1500 μm, respectively. For each simulation, the copper wires were assumed to be perfect electric conductors (PEC) with the waveguide's transverse section being "surrounded" by a rectangular, metallic boundary condition. Note that in order to calculate the eigenmodes of the two wire waveguides with different wire separations, the metallic boundary must be far apart from the wires (for example, as much as 2000 μm), in order to avoid the unnecessary standing wave solution due to the chosen modeling configuration. For 300 μm separation between the wires, the TEM mode is mostly concentrated between the wires, whereas for a 500μm separation, the electric field is now

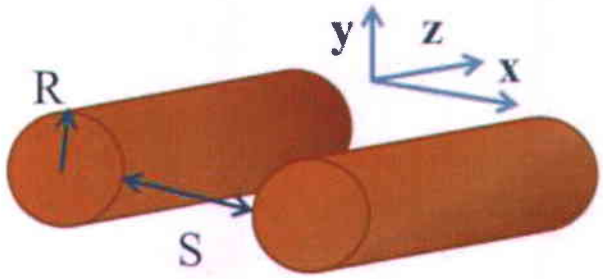

Fig. 2.1 Scheme of a two-wire waveguide with separation S and radius R. The two-wire mode lies in the **x-y** plane and the mode propagates is in the **z** direction.

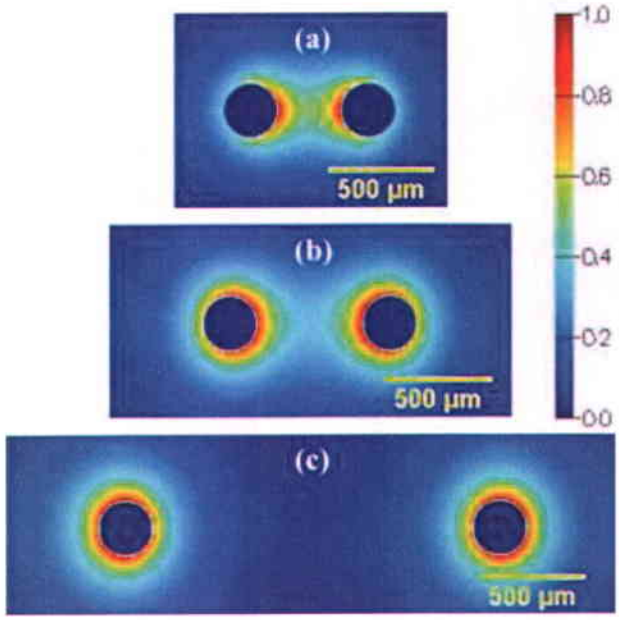

Fig. 2.2 Mode distribution of a 1 THz wave in a two-wire waveguide with a wire radius of 125 µm and a wire separation of (a) 300 µm, (b) 500 µm and (c) 1500 µm.

more concentrated close to the metal surface. With further increase in the separation between the wires (1500 µm), the two-wire waveguide loses the property of supporting a linearly polarized TEM mode for the desired wavelength of operation as it now tends to carry an azimuthally (or radially) polarized Sommerfeld mode in each wire.

Commonly used THz sources, such as PC antennas, emit radiation in a linearly polarized mode that is very similar to the dipole like TEM mode of the two-wire waveguide. A single wire waveguide, however, carries a radially polarized mode (or Sommerfeld mode). As a result, the TEM mode of a two-wire waveguide is relatively easier to excite with a PC antenna in comparison to the Sommerfeld mode of a single wire waveguide. Also the two-wire waveguide has low bending loss as compared to a single wire waveguide [71]. This is owing to the fact that, Sommerfeld mode gets coupled to free space easily, on bending.

In a seminal work [71], the TEM mode distribution of a two-wire waveguide was experimentally reported for wires made of stainless steel with wire separation S = 4.7 mm and radius R = 150 µm. The authors mapped the electric field around the waveguide's transverse section and observed that the field distribution resembles a dipole pattern (see Fig. 2.3). However, due to the very large separation between the wires, the observed bandwidth for the

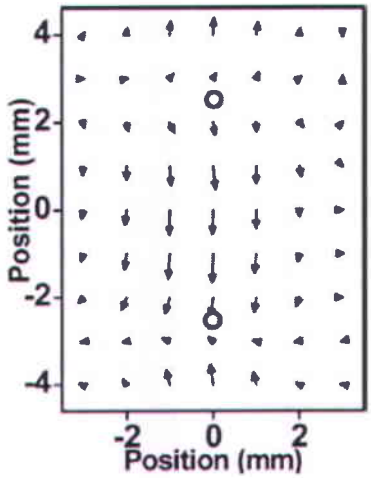

Fig. 2.3 Dipole like field distribution in the two-wire waveguide with distance between the two wires of 4.7mm [71].

TEM mode of the two-wire waveguide was < 0.5 THz (> 0.6 mm in wavelength) [71]. They also reported tenfold smaller bending losses in two-wire waveguides in comparison to a single wire waveguide for the same angle of bending. This experiment demonstrated the strong confinement of THz radiation in a two-wire waveguide in comparison to a single wire where the THz radiation is weakly coupled.

Recently a theoretical study on two-wire waveguides in a composite structure [75] was carried out in order to address the issue of handling the two-wire structure. They report that the addition of hollow dielectric cladding around the structure induces more loss and dispersion compared to the classical two-wire structure with the same parameters. This problem could be solved by increasing the air region around the two-wires. The two-wire waveguide discussed in this chapter avoids the above issues as it is devoid of any dielectric cladding.

2.2 Waveguide model

The two-wire waveguide, studied in this thesis, consists of two copper wires of 125 μm radius with a separation S = 300 μm (see Fig. 2.4). This length of separation between the wires, results in a broadband THz transmission (> 2 THz) through the waveguide [60].

2.2.1 Challenges and solutions for waveguide design:

In the initial design for the waveguide, the major challenge was to hold the two wires as close as 300 μm apart in free space, i.e. in a gas (Fig. 2.4). It was initially proposed to place the two wires in a dielectric support, but this would have led to dispersion and attenuation of the THz signal.

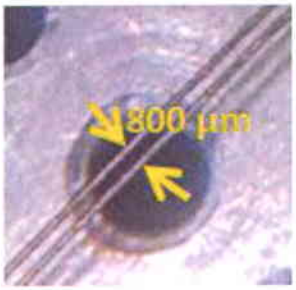

Fig. 2.4 Photograph of the two wire waveguide consisting of two copper wires of 250 µm diameter separated by 300 µm in free space.

The dielectric support would have also nullified the special characteristics (low-dispersive TEM mode) of the two-wire waveguide. The devised solution consists in holding the wires under tension in free space. The proposed design involves a metallic base plate acting as the backbone of the waveguide structure, as shown in Fig. 2.5. Two polymer slabs were then attached to either end of the metallic base plate. A hole of 800 µm diameter each was drilled through the centre of the polymer slabs. The two wires were then passed through the holes. The four free ends of the wires were then attached to four screws, which were fixed to the metallic base plate. These screws were used to pull the wires in order to apply a tension on them and thereby keep them uniformly apart. As the holes were of 800 µm diameter each and the wires used were of 250 µm diameter, a separation of 300 µm was achieved. The total length of the designed two-wire waveguide is 20 cm.

2.3 Addressing coupling issues

Coupling THz radiation into a two-wire waveguide has been numerically studied by

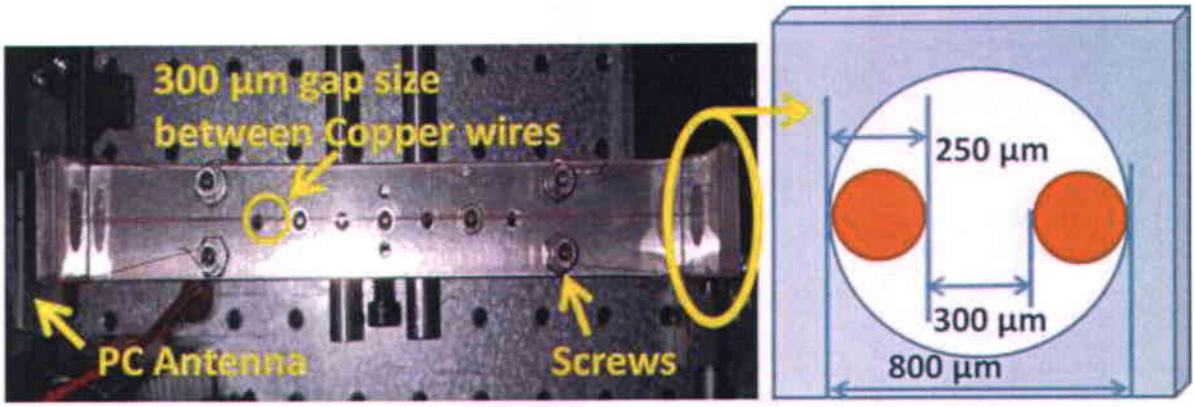

Fig. 2.5 Designed two-wire waveguide structure with the schematics of the arrangement used to keep the wire separated in air by 300 µm.

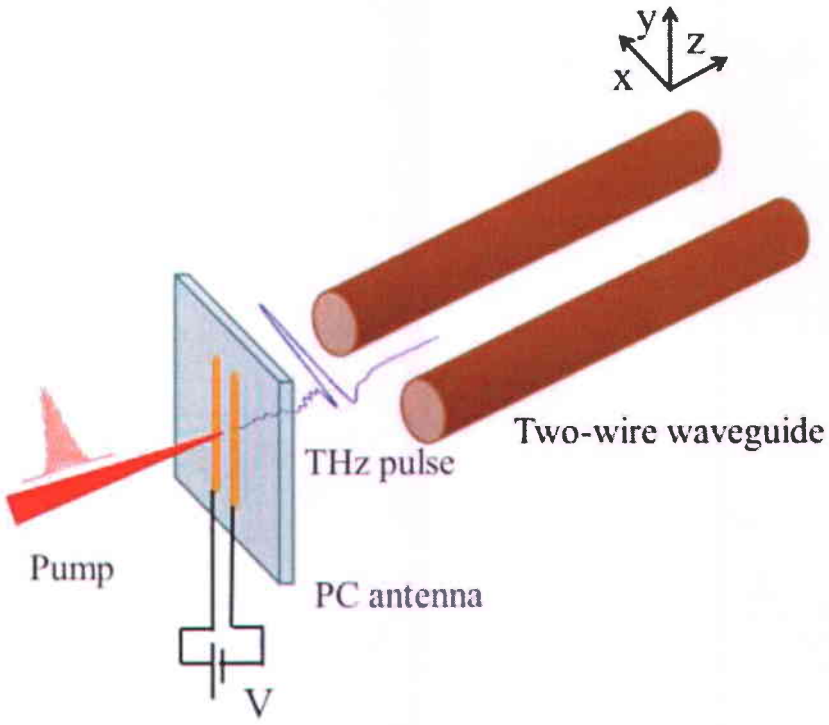

Fig. 2.6 Coupling scheme for the two-wire waveguide lying on x-z plane, with its transverse section perpendicular to z direction. The THz pulse is polarized in the x direction.

independently using a metallic parallel plate waveguide and a single dipole in reference [76] and by end fire coupling method in reference [60]. In reference [60], it was pointed out that, in order to achieve maximum efficiency in coupling THz radiation into the two-wire waveguide, the Gaussian beam waist should be equal to the wire separation. Achieving a beam waist of 300 μm for an optimum transmission around 1 THz is challenging due to the diffraction limit criterion. Hence, in order to overcome this issue, a PC antenna without a hyper-hemispherical lens was placed close to the input end of the waveguide. This configuration allowed us to achieve an end butt coupling condition and can be compared to the coupling achieved by a single dipole source, as described in reference [76]. There is an essential factor to consider for coupling THz radiation into the waveguide: the polarization of the THz radiation emitted by the PC antenna must be parallel to the plane joining the two wires (see Fig. 2.6).

2.4 Experimental setup

The experimental setup used to characterize the waveguide is based on the principle of THz-TDS as illustrated in Fig. 2.7. For the experiment we used a Ti:Sapphire based femtosecond laser

source with 80 MHz repetition rate and 125 fs pulse duration. The laser beam from the femtosecond laser is then split into two parts: pump and probe. The pump beam carries about 150 mW of power and the probe beam carries a power of less than 10 mW.

Generation:

The pump beam is directed into the THz generation system of the setup. It consists of a coplanar stripline based PC antenna with a separation of 120 µm in between the electrodes lines. There is no hyper-hemispherical lens attached to the back of the antenna. THz radiation is generated when a square wave voltage of 60 V is applied on the electrodes and the pump beam is focused onto the PC antenna (details on THz generation by a PC antenna were already discussed in section 1.1.2). In order to focus the pump beam onto the PC antenna, a lens (L1) with a focal length of 5 cm was employed. The relative spot size was measured to be ~50 µm. The THz radiation generated in this part of the setup is collected by the 1st parabolic mirror (PM1) as shown in Fig. 2.7.

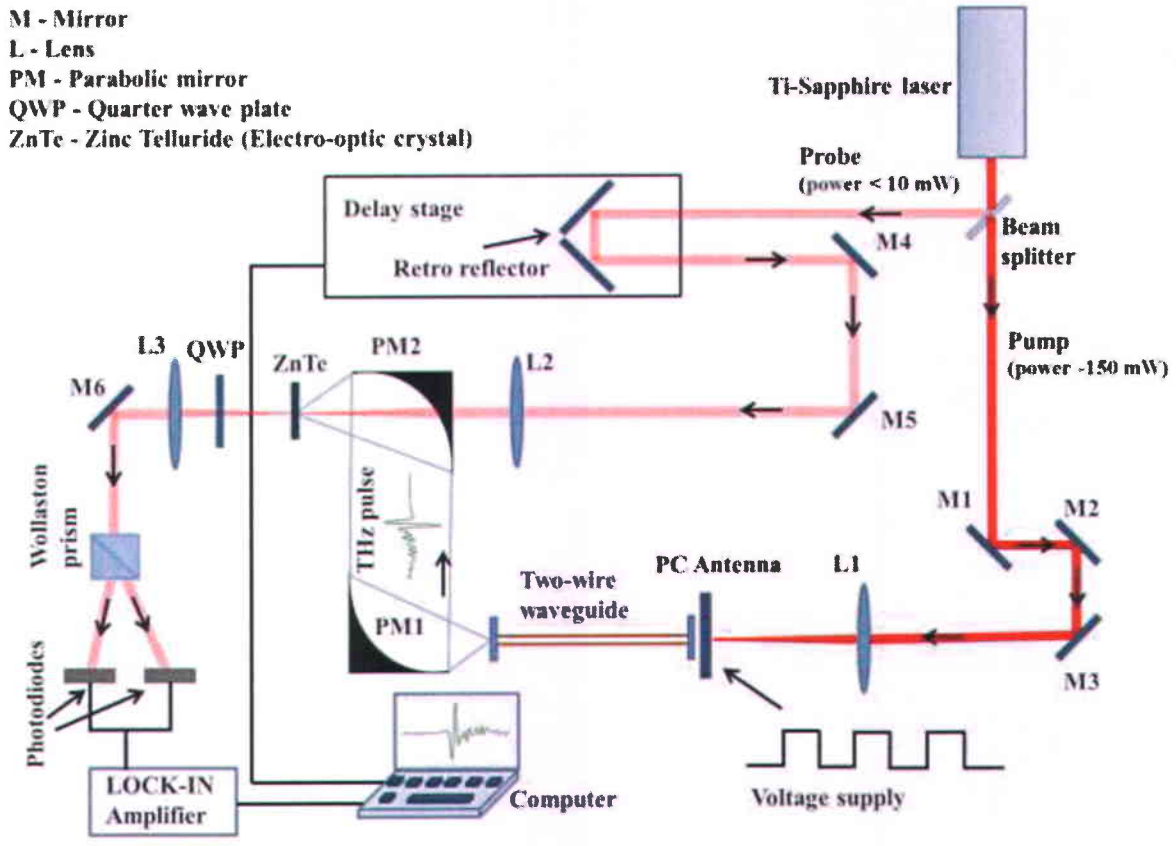

Fig. 2.7 Experimental scheme for the THz waveguide characterisation.

Detection:

The probe beam is then directed into the detection system. The detection system is based on electro-optical sampling. A <110> grown ZnTe crystal of 2 mm thickness is used as the electro-optic crystal. The probe beam passes through a hole drilled into the 2nd parabolic mirror (PM2), which focuses the THz beam collimated by PM1 onto the ZnTe crystal. In the ZnTe crystal, the probe beam interacts with the THz radiation where it undergoes modulation in its polarization. It then passes through the quarter wave plate (QWP) as discussed in section (1.1.2). A Wollaston prism splits the probe beam into two perpendicularly polarized components s and p. The intensities of the two perpendicularly polarized beams are detected by a pair of photodiodes. The difference between the intensities of the two beams is measured by a lock-in amplifier. A computer program records the difference in intensities and also controls the delay stage shown in Fig. 2.7. The delay stage carrying the retro-reflector is used to induce a time delay between the THz pulse and the probe pulse. In this way the THz electric field can be mapped over the required time scan. As an important note, the lock-in amplifier used for the measurements is locked on to the frequency of the PC antenna's voltage supply. This helps to remove the background noise in our measurements.

In our experimental setup, the detection system is fixed. In order to measure the signal generated by the PC antenna, the latter is placed at the focus of PM1. The PM1 collimates the generated THz beam and directs it to the PM2. The PM2 focuses the THz radiation on to the detection crystal. Similarly, in order to detect the signal carried by the 20 cm waveguide, the output end of the waveguide is placed at the focus of PM1. In order to efficiently couple THz radiation into the waveguide, the PC antenna is placed close (~4 mm of air gap) to the input end of the waveguide as shown in Fig. 2.7.

Challenge of THz absorption in ambient air

In this paragraph, we discuss the challenge of THz absorption by water vapour in ambient conditions. Figure 2.8 (a-b) shows the signal from the waveguide and its power spectrum, in an unpurged environment. The oscillations observed after the main THz pulse (see Fig. 2.8 (a)) are due to the absorption of THz radiation by water vapour in air. Water, being a polar molecule, plays an active role in THz absorption due to molecular rotations in its ground vibrational states [77]. The absorption lines of water vapour in the THz range are indicated by the dashed lines in

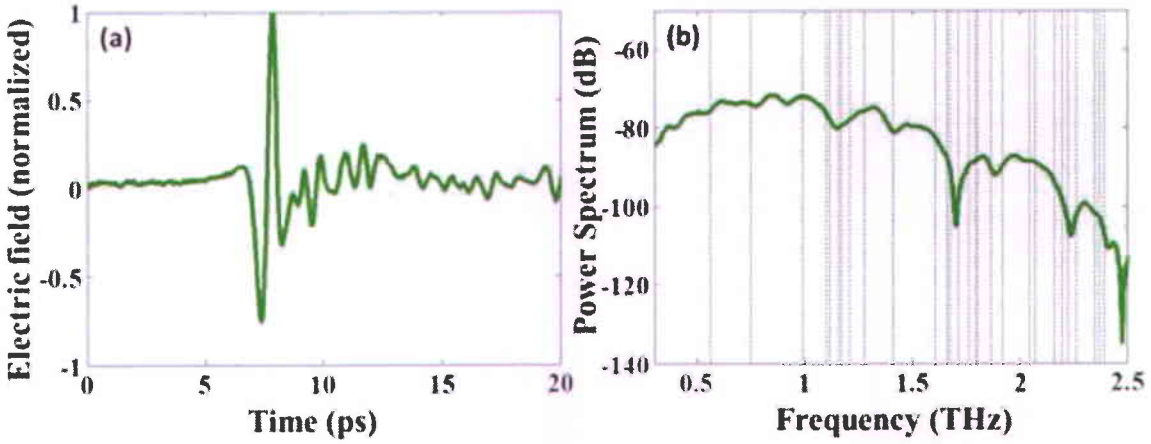

Fig. 2.8 (a) THz signal from the 20 cm long two-wire waveguide in ambient air and (b) its spectrum, where the dashed lines represent water absorption lines. All curves are normalized to their peak.

Fig 2.8 (b) and can be found in the literature [77, 78]. However, these absorption lines are not clearly resolvable due to a short THz propagation length of 45 cm (including inside and outside the waveguide) and low relative humidity (33%) of the environment during the measurement. The presence of water vapour leads to the attenuation of the propagating THz radiation and also to the distortion of the THz pulse. This was a major challenge in our experiments, and we overcame it by purging our experimental setup.

2.5 Experimental results and discussion on the two-wire waveguide

The experiments on the two-wire waveguide were carried out in a purged environment (nitrogen filled environment with 0% relative humidity) to overcome absorption of THz radiation by water vapour. The experimental results show a low-dispersive broadband propagation of THz radiation through the developed two-wire waveguide. The reference signal, i.e. the THz temporal signal generated by the PC antenna, and its power spectrum are shown in Fig. 2.9 (a) and (b), respectively. Similarly, the THz temporal signal from the two-wire waveguide and its power spectrum are shown in Fig. 2.9 (c) and (d), respectively. On comparing Fig. 2.9 (a) and Fig. 2.9 (c) it can be observed that the sub-picosecond, single cycle nature of the reference signal is maintained after propagation through the waveguide. This shows that the THz pulse has propagated through the two-wire waveguide with negligible group velocity dispersion (GVD). On comparing Fig. 2.9 (b) and 2.9 (d), it can be observed that the waveguide has also successfully carried a broad spectrum (>2 THz) as emitted by the PC antenna. These results

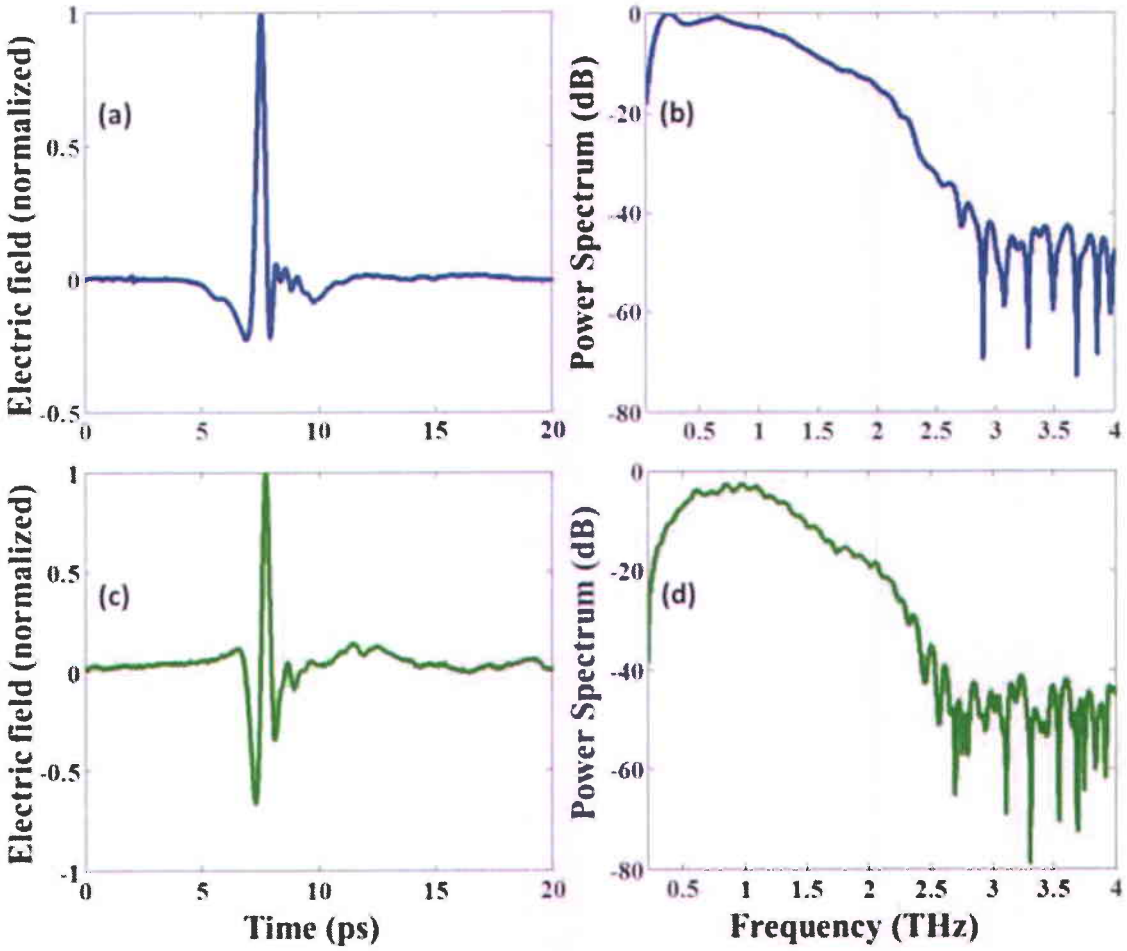

Fig. 2.9 (a) THz signal emitted by the PC antenna in a purged setup and (b) its spectrum. (c) THz signal from the 20 cm long two-wire waveguide in a purged setup and (d) its spectrum. All curves are normalized to their peak.

demonstrate that the developed waveguide can transmit broadband THz pulses with negligible dispersion and without any broadening.

2.6 Conclusion

In this chapter, we provided a theoretical introduction on the two-wire waveguide. Such waveguides carry a TEM mode when the separation between the two wires is close to the operating wavelength. A separation of 300 μm between the wires resulted in the transmission of THz radiation around 1 THz with a good confinement of the radiation in the air space between the wires. This two-wire waveguide was experimentally realized and its property has been investigated for THz radiation over a bandwidth of more than 2 THz. The tested waveguide has

also shown low-dispersive propagation over the investigated bandwidth. Such waveguides with low dispersion and broadband propagation open up new avenues for THz interconnects. Also, the easy accessibility of the guiding region facilitates insertion of designed structures to perform signal processing. This idea is developed in the next chapter (Chapter 3), which discusses about a polymer grating being inserted in the two-wire waveguide. The grating structure enables frequency filtering of the THz signal.

Chapter 3: Bragg gratings in two-wire waveguides

3.1 Introduction: Bragg gratings

A Bragg grating can be defined as a periodic perturbation of the refractive index in a medium. It can be compared to a 1D photonic crystal. Bragg gratings were first developed for optical fibers by K. O. Hill in 1978 at Canadian Communication Research Centre (CRC), Ottawa, Canada. Since then, fiber Bragg gratings have found broad range of applications such as sensing [79], structural health monitoring [80], dispersion compensation [81], etc. A general pictorial overview of an optical fiber based Bragg grating is shown in Fig. 3.1.

Bragg gratings have also been a key component for optical signal processing in the field of fiber optic telecommunications namely band rejection [82], wavelength selective devices [83, 84], temporal optical differentiators [85], temporal optical integrators [86], pulse shapers [87], etc. These applications have been achieved by designing fiber Bragg gratings with a desired transmission function. Therefore, it is expected that Bragg grating structures have potential application in the THz regime, as for example in the fields of sensors and frequency filters for future THz communication networks. The basic working principle of a Bragg grating is based on a simple phase matching condition given by:

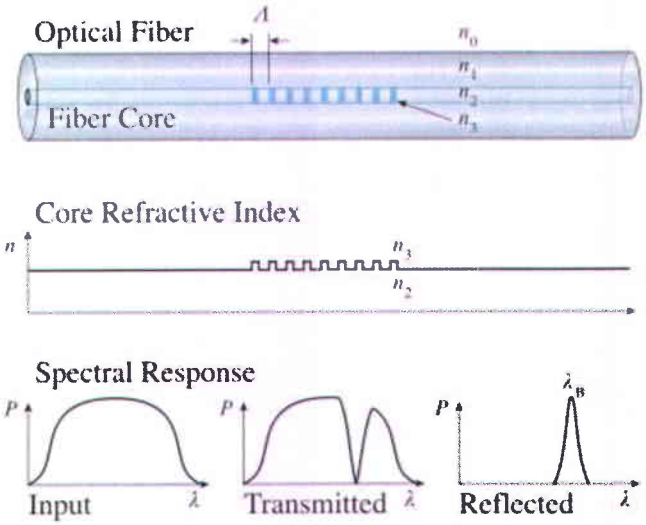

Fig. 3.1 Optical fiber based Bragg grating with the refractive index variation and spectral response (Figure source [88]).

$$\Delta\beta = \beta_\mu \pm \beta_\nu - \frac{2\pi}{\Lambda} = 0 \tag{3.1}$$

where β_μ and β_ν represent the propagation constants for the counter propagating modes in the waveguide and Λ is the period of the grating. Such a grating can also be inserted in a THz waveguide in a way similar to a Bragg grating in fibers. In this chapter, we will demonstrate THz frequency filtering in our two-wire waveguide geometry by using a polymer based Bragg grating. The investigated device could be used in future THz communication networks.

3.2 Periodic structures in THz waveguides

An important application in any kind of waveguides is signal processing and sensing. With the use of a THz-TDS setup, researchers have characterized the amplitude and phase response of different photonic crystal structures in a waveguide geometry like the PPWG [89-93]. These experiments hold promises for future THz communication systems. For example, by using photonic crystals, a wide band gap from 0.6 to 1.55 THz, with a transmission contrast of 90 dB, and a band rejection with a contrast of approximately 60 dB around 1.692 THz has been observed in two different samples [90]. In another seminal work [94], a very high Q of 430 at 2.996 THz among the other observed resonant frequencies was reported by using 1D gratings in a PPWG. This makes such a waveguide a good candidate for sensing applications. Owing to the necessity of developing frequency filtering, a grating based on paper (insertion loss ~17 dB) [95] was very recently demonstrated in a two-wire geometry. This two-wire waveguide has a wire separation of 900 μm and a bandwidth up to 1.5 THz. We report here the possibility to perform frequency filtering using a polymer grating in our broadband two-wire waveguide, with a frequency notch > 20 dB. The polymer grating discussed in this thesis is based on extruded polyethylene and will be described in the next section.

3.3 Description of the polymer Bragg grating used for frequency filtering

We used a polymer Bragg grating (shown in Fig. 3.2) for demonstrating frequency filtering in our two-wire waveguide. The Bragg grating is developed from a commercially available and easy to implement polymer mesh made of extruded polypropylene (model no, 9275T27, Mc Master Carr), consisting of horizontal and vertical polymer rods in a woven fashion. To obtain the Bragg grating structure from the polymer mesh, we removed the horizontal set of rods. The

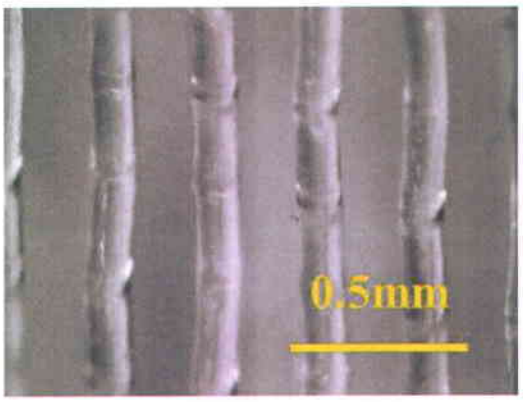

Fig. 3.2 Photograph of the polymer Bragg grating comprising of polymer rods used for achieving frequency filtering in the two-wire waveguide.

measured diameter of these rods was 110 ± 2 μm and the measured spacing between the rods was 137 ± 2 μm. As a result, the period of the grating was measured to be ~ 247 μm. For the experiment, we took 16 periods of the grating, which amounts to an approximate length of 4 mm.

3.4 Experimental results on the polymer Bragg grating in a two-wire waveguide

In order to analyze the effects of the grating on the THz signal, the reference signal from the waveguide without the grating and the signal after the grating was inserted were measured. The measured temporal signals are shown in Fig. 3.3 (a). As observed in the figure, the peak amplitude of the signal gets somewhat delayed due to insertion of the grating which increases the

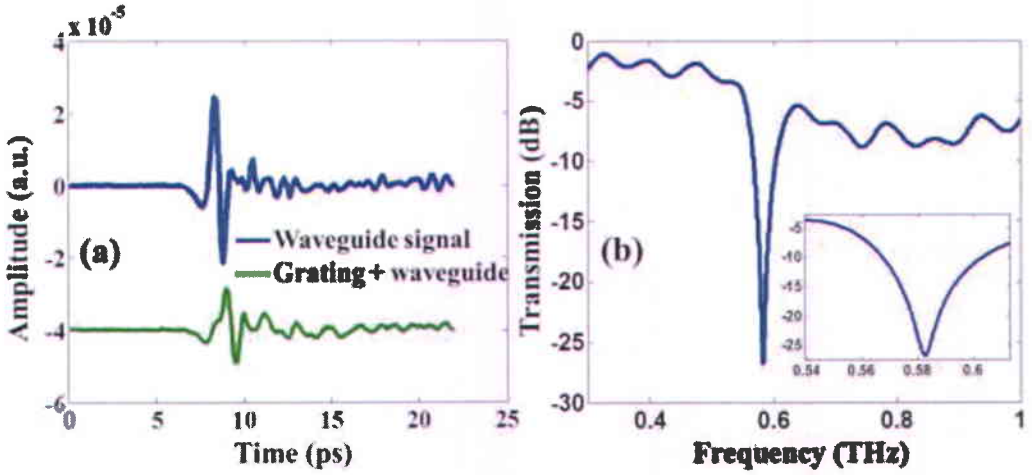

Fig. 3.3 (a) Signal from the waveguide (blue) and with the grating inserted in it (green) (b) Transmission Spectrum of the signal detected after inserting the grating in the waveguide with the inset showing a close view of the dip.

average refractive index of the waveguide. The transmission spectrum of the grating is shown in Fig. 3.3 (b) with the inset showing a close view of the dip in the transmission spectrum. From the spectrum it is observed that the insertion loss for the grating varies from 1 dB to 7 dB from 0.3 to 1 THz. A fine notch of about 23 dB was observed at 0.5823 ±0.0003 THz with a line width of ~16 GHz.

Finite difference time domain method (FDTD) based simulation results

Besides conducting experiments, we also calculated the position of the dip in the grating's spectrum by using the finite difference time domain (FDTD) method through the commercial software Lumerical FDTD. Figure 3.4 (a) shows a snapshot of the FDTD simulation setup being carried out. The simulation involved a perfectly matched layer (PML) boundary that encloses the simulation area comprising the waveguide, the Bragg grating and the THz single dipole source. The PML boundary does not allow the electromagnetic radiation leaving the simulation region to reflect back as it may alter the simulation results. For our FDTD simulation we neglected the absorption coefficient of the polymer and only considered the real part of the refractive index of polypropylene, which is 1.51 [7]. For the simulation we also considered the metallic wires as perfect electric conductors. A time monitor as shown in Fig. 3.4 (a) records the time varying electric field of the THz pulse (generated by the single dipole source) after passing through the Bragg grating. The power spectrum of the THz pulse thereby recorded by the time monitor is shown in Fig. 3.4 (b). The power spectrum from the FDTD simulation predicted the dip in the

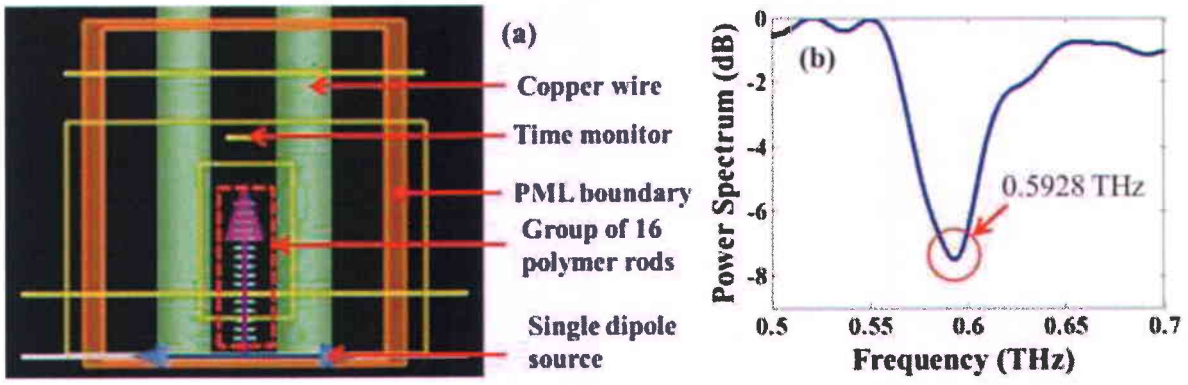

Fig. 3.4 (a) Snapshot of the FDTD simulation setup (top view) of the polymer Bragg grating inserted in the two-wire waveguide. (b) Power spectrum of the grating response recorded by the time monitor in the FDTD simulation with the dip at 0.5928 THz.

grating's response to be at 0.593 ± 0.001 (see Fig 3.4 (b)) which is in close agreement with the experimental results.

We have hence shown that by inserting a Bragg grating structure with thickness less than the spacing between the wires and utilizing the low-dispersion of the waveguide, we can achieve spectral filtering and thereby modulate the THz pulse. As a consequence, the two wire waveguide appears to be a promising candidate for future THz interconnects with integrated signal modulation.

3.5 Enhancement of a water line

In this section, we discuss our observations concerning the enhancement of a water line at 0.557 THz. This enhancement is due to the occurrence of slow-light at the band edge of the polymer grating. Several discussions on slow-light can be found in the literature. Slow-light occurs in various contexts such as Electromagnetically Induced Transparency (EIT) [96], coherent population oscillations [97, 98], Stimulated Brillouin Scattering (SBS) [99-101], resonances in coupled ring resonators [102], plasmonic structures [103, 104], photonic crystals [105, 106] and Bragg gratings (1D photonic crystal) [107, 108]. Slow-light occurs near the edge of the absorption or reflection band. For example, in photonic crystals, slow-light occurs at the band edges (see references [105, 106]). The same physical principle can be used to explain slow-

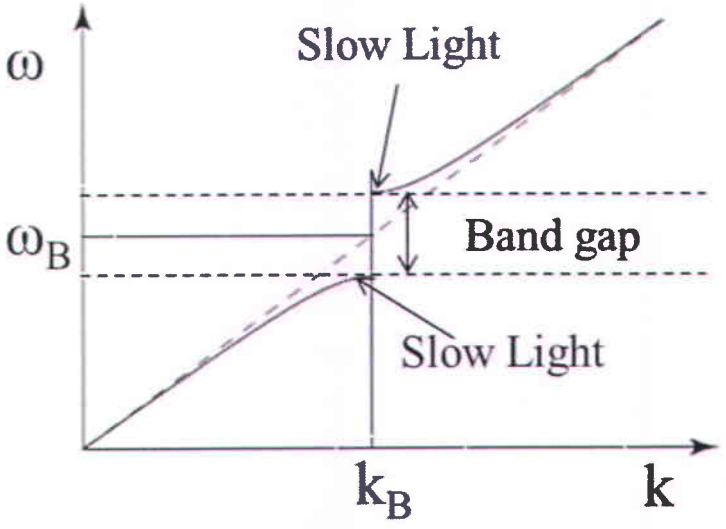

Fig. 3.5 Dispersion curve of a Bragg grating structure with Bragg frequency ω_B showing its band gap and indicating the region of slow-light formation near its band edge (adapted from [109]).

light in fiber Bragg gratings (also acting as 1D photonic crystal). Figure 3.5 shows the dispersion curve of a fiber Bragg grating with Bragg frequency ω_B. The group velocity ($d\omega/dk$) of the propagating pulse decreases in the vicinity of the band edge of the Bragg grating, leading to the formation of slow-light as indicated in Fig. 3.5. This phenomenon could find applications in realizing optical buffers, optical memory storage devices and in increasing computing speed. Another application of slow-light, as reported in literature, is to realize sensors with enhanced sensitivity [108].

In this thesis, we have employed a polymer Bragg grating inside the waveguide for frequency filtering. The water line at 0.557 THz, lying close to the band edge of our Bragg grating, was observed to be enhanced when the grating was inserted in the two-wire waveguide. The blue curve (grating's spectrum in the waveguide for an unpurged setup) in Fig. 3.6 shows the enhancement of this water line (dashed line), which lies close to the band edge of the grating. The red curve represents the THz spectrum of the radiation propagating in the waveguide without the grating in an unpurged environment. It is important to note here that the measurements for the blue and the red curves were taken in the same humidity conditions. The green curve represents the grating's spectrum in the waveguide for a purged (relative humidity of 0%) environment. Hence, this absorption enhancement is most probably due to the increased

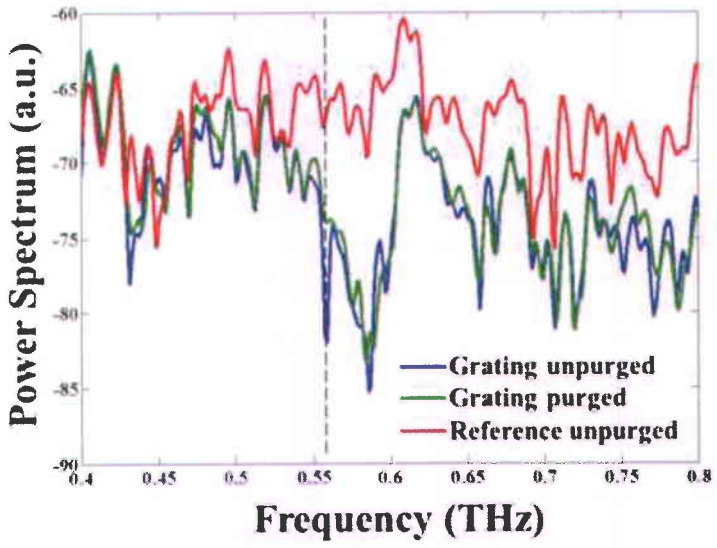

Fig. 3.6 Enhancement of water absorption at 0.557 THz (dashed line) as shown by the blue curve (grating spectrum in unpurged conditions). The red curve indicates the waveguide signal spectrum in ambient conditions (unpurged) and the green curve shows the grating spectrum in purged conditions.

interaction between THz and water vapour in the ambient air due to the slowing down of the THz pulse propagating inside the waveguide near the band edge of the Bragg grating under investigation. To observe the phenomenon, a time window of 165 ps was considered in our THz-TDS experiments so that the long oscillatory trail in the THz pulse due to water absorption could be taken into account.

3.6 Conclusion

In this chapter, frequency filtering in the two-wire waveguide has been demonstrated. This has been achieved by inserting a grating made of polymer rods in the guiding region. One of the benefits of such a waveguide is the easy accessibility to the THz confinement region as it opens up opportunities for manipulating the signal and carrying out desired signal processing in the waveguide. Thus the two-wire waveguide could serve as an important component for future THz communication networks. In addition, we report an enhancement of the water absorption line at 0.557 THz, upon insertion of our Bragg grating inside the waveguide. This enhancement is observed due to occurrence of slow-light at the band edge of the polymer Bragg grating.

Chapter 4: Two-wire THz transmitter

4.1 Introduction

As mentioned in the previous chapter, the proposed two-wire waveguide has a potential to serve as interconnect in future THz communication networks and enhanced THz-TDS. For the experiments conducted in this thesis and described above, the THz radiation was coupled into the waveguide by bringing the input end of the waveguide very close to the PC antenna. Achieving coupling in such a configuration is quite complicated experimentally, as both the waveguide and the antenna have to be aligned. In this passive waveguide configuration, it can be assumed that the THz radiation is being coupled into the waveguide from free space. However, a large fraction of this free space THz radiation, emitted by the PC antenna, is not coupled into the waveguide and the low, far-field mediated coupling efficiency of the system strongly limits its applicability. Hence, in order to increase the coupling efficiency, we propose to generate THz radiation directly inside the waveguide. We achieved THz generation by illuminating a thin rectangular piece of GaAs (width × breadth × height: 300 μm × 300 μm × 5mm,inserted in between the two metallic wires of the waveguide) with femtosecond pulses and simultaneously applying a voltage to the wires. This "active waveguide" structure (we also call it as a "two-wire THz transmitter") is comparable to a PC antenna where the wires act as electrodes and the GaAs piece acts as the semiconductor substrate. The THz radiation after being generated in the GaAs piece gets directly coupled into the waveguide. Figure 4.1 (a) and (b) shows the schemes of the passive waveguide (two-wire waveguide coupled to an external PC antenna) and of the active waveguide, respectively. Note that the external PC antenna is made of the same GaAs piece used to fabricate

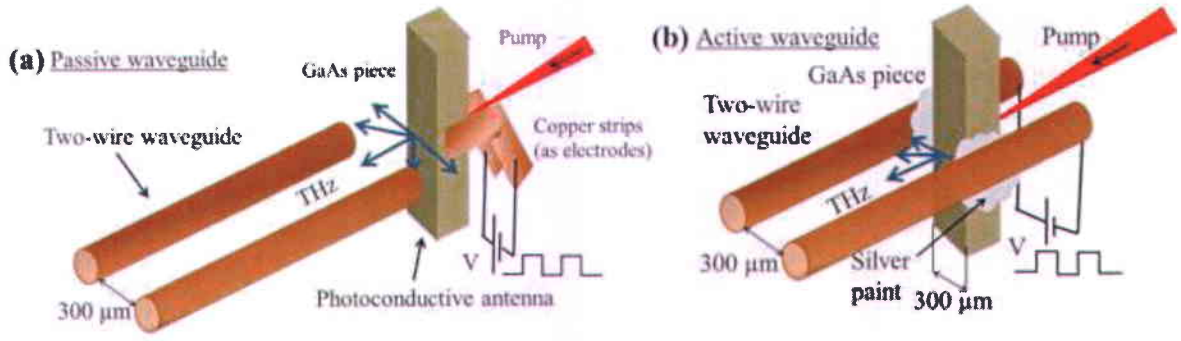

Fig. 4.1 Schematics of the (a) passive and (b) active waveguide. The arrows denote the direction of THz radiation emitted from the GaAs piece.

the active waveguide. In order to increase the contact efficiency between the GaAs piece and the copper wires of the waveguide, a layer of silver paint is applied at the wire and the GaAs junction.

With the structure described above, a more efficient coupling between the source and the waveguide is expected. The two-wire THz transmitter has the potential to achieve THz generation, propagation and pulse modulation, all in one waveguide. Such a concept is extremely appealing, as it would decrease the losses due to coupling at the input side of the waveguide and avoid the use of intermediate signal processing components.

4.2 Experimental results and discussions

For our preliminary experiments, we used a two-wire waveguide of length 10 cm. For all the experiments, a pump power of 220 mW and a voltage of 110 V were applied onto the GaAs piece. We first demonstrated that the GaAs piece between the two wires could be used in a PC antenna configuration (see the external PC antenna in Fig. 4.1 (a)). Figure 4.2 (a) and (b) shows the temporal THz signal and the power spectrum, respectively, generated by the external PC antenna. The THz signal and spectrum shown in Fig. 4.2 are normalized to their respective peaks. Then, the two-wire waveguide of 10 cm length was coupled to the external PC antenna (passive waveguide configuration). Here the PC antenna and the waveguide are separated by a small air gap as shown in Fig. 4.1 (a). Figure 4.3 (a) and (b) show the observed temporal signal and spectrum, respectively, measured at the end of the 10 cm waveguide. Finally, the same piece of GaAs was inserted in between the two wires of the 10 cm long waveguide (active waveguide configuration). The observed temporal signal and spectrum of this two-wire THz transmitter are shown in Fig. 4.4 (a) and (b) respectively. Note that the temporal THz signals in Fig. 4.3 (a) and 4.4 (a) are normalized to the peak of the PC antenna's temporal signal and their spectra in Fig. 4.3 (b) and 4.4 (b) are normalized to the peak of the PC antenna's spectrum. As can be observed from Fig. 4.2, the piece of GaAs acts as an external PC antenna, generating a single cycle THz pulse over 2 THz of bandwidth. By comparing Fig. 4.3 (a) and 4.4 (a), we observe that the peak signal strength is almost five times higher in the active configuration as compared to the passive counterpart. Hence, this experiment demonstrates that the peak THz field delivered by the active two-wire THz transmitter (Fig. 4.4) is higher in magnitude than the two-wire waveguide being coupled to an external PC antenna (Fig. 4.3).

The shape of the THz pulse measured at the end of the 10 cm two-wire THz transmitter is not a single cycle, contrary to expectation (see Fig. 4.4 (a)). This shape of the THz pulse needs to be further investigated theoretically. Indeed, one of the main sources of distortions seems to be the extended electrodes length along the propagation direction. Theoretical studies and further experiments should be carried out to provide insight into the preliminary experimental results and improve signal quality.

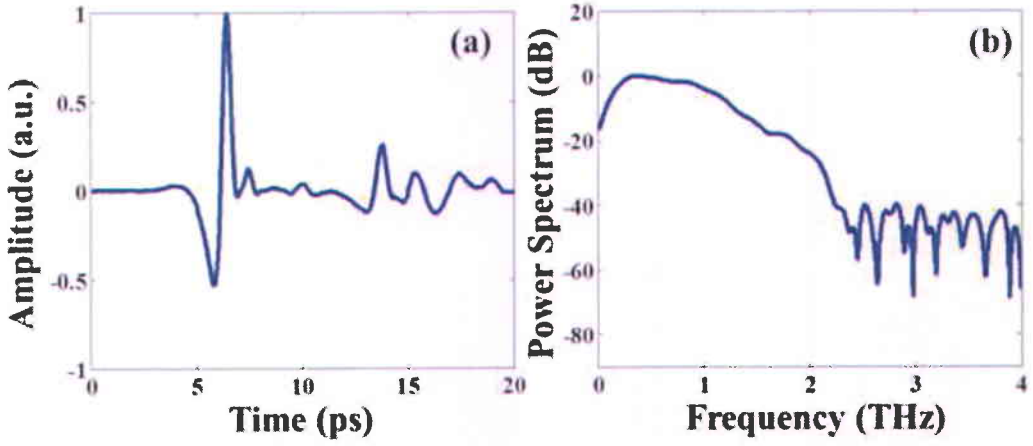

Fig. 4.2 GaAs piece used as a PC antenna: (a) signal, (b) power spectrum. All curves are normalized to their peaks.

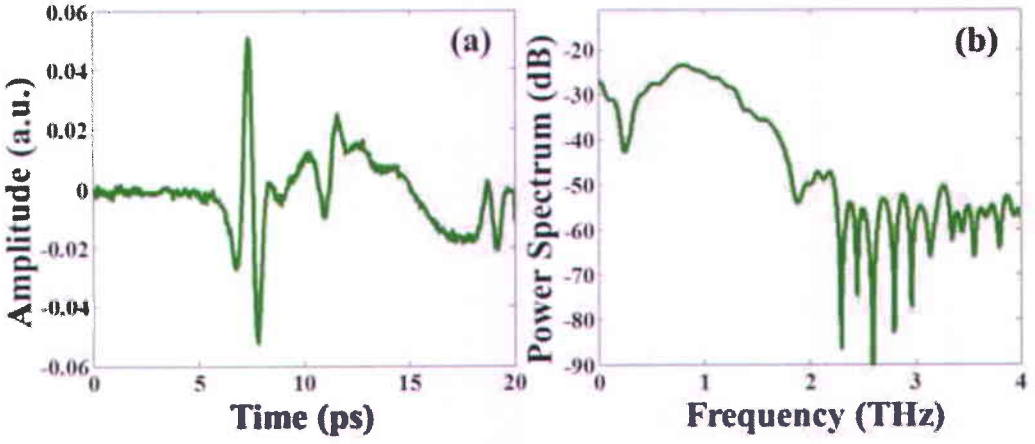

Fig. 4.3 (a) Signal from the 10 cm waveguide with GaAs piece being used as an external PC antenna (normalized to the peak of the PC antenna's signal) and (b) its power spectrum (normalized to the peak of the PC antenna's spectrum).

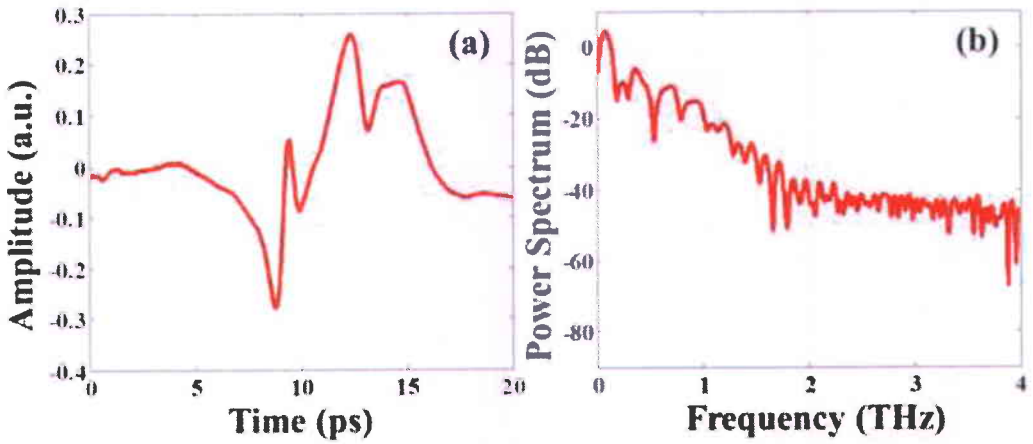

Fig. 4.4 (a) Signal from 10 cm waveguide with GaAs piece inserted between two wires (normalized to the peak of the PC antenna's signal) and (b) its power spectrum (normalized to the peak of the PC antenna's spectrum).

4.3 Conclusion

In this chapter we addressed the issue of poor coupling efficiency in our passive two-wire waveguide by introducing a novel active waveguide design, in which the generation of THz signal occurs directly in the guiding structure. We fabricated the active waveguide by inserting a thin rectangular piece of GaAs with a width and breadth of 300 μm in between the two wires of the waveguide. The active waveguide structure is comparable to a PC antenna where the wires of the waveguide act as the electrodes and the GaAs piece acts as the semiconductor substrate. The active waveguide structure, which we also named as "two-wire THz transmitter", when developed efficiently could be an essential component in future THz communication networks and THz-TDS. Exploiting the tightly confined TEM mode of a two-wire waveguide, a signal processing component can be inserted in between the two wires of the transmitter to realize a THz source with inbuilt pulse shaping characteristics.

Chapter 5: Conclusion and future perspective

The field of terahertz (THz) radiation is evolving quickly and is leading to a plethora of scientific and technological developments. It has found very useful applications in the field of imaging, security and spectroscopy. Terahertz radiation is shorter in wavelength than microwaves and has the ability to pass through several dielectric materials, unlike infrared radiation. The spectral signature of several organic and inorganic molecules falls in the THz frequency range. These characteristics make the field of THz very exciting and interesting to study. Another field where THz technologies can play a significant role is communications and data transfer. The current wireless communication system, which is based on microwave radiation, faces an ever-increasing demand for faster transfer rates. One possible way to solve this problem would be to move to higher frequency region such as THz, which could provide larger bandwidth for higher information transfer rates. In order to realize the goal of a future THz communication network, special waveguides and signal processing components need to be developed and investigated.

Therefore, as a further step towards a future THz communication network, a low-dispersive THz two-wire metallic waveguide was developed and characterized in this thesis. The two-wire waveguide (wire radius of 125 μm and wire separation of 300 μm) carries a low-dispersive TEM mode when the wire separation is close to the wavelength of operation. In addition, the TEM mode carried by the two-wire waveguide is linearly polarized, similar to the radiation emitted by conventional PC antenna sources. Hence, the two-wire waveguide mode is easier to excite by PC antennas in comparison to the radially polarized modes of a single wire waveguide for THz.

In our experiments, we demonstrated the propagation of single cycle THz pulses in the two-wire waveguide over a bandwidth of 2 THz. The waveguide was found to carry the entire spectrum generated by the PC antenna source. This demonstrated the broadband nature of the developed two-wire waveguide.

The developed two-wire waveguide gives an easy access to its guiding region. As a result, a polymer Bragg grating could be inserted between the two wires and a frequency filter has been realized. Thanks to the slow-light effect enabled by the grating, we also observed an enhancement in the water line at 0.557 THz.

Finally we also reported for the first time an active, two-wire THz waveguide. We realized the active waveguide by illuminating a thin rectangular piece of GaAs inserted between

the two metallic wires of the waveguide with femtosecond pulses and by applying voltage on the wires. The active waveguide structure can be compared to a PC antenna where the wires act as the electrodes and the thin piece of GaAs acts as the semiconductor substrate. The THz signal thereby generated in the GaAs piece is directly coupled into the two-wire waveguide. With this active waveguide, we observed a THz signal, whose peak electric field was higher than that of the two-wire waveguide coupled to an external PC antenna. This experiment shows that our two-wire waveguide can be used as a THz transmitter as well. Such an active waveguide carries a higher strength associated to the THz field as compared to the waveguide coupled to an external source.

The two-wire waveguide possesses special characteristics, such as low-dispersion propagation and a relatively tight confinement of THz radiation in the region between the wires. These features make the two-wire waveguide a potential candidate for future THz communication networks, enhanced THz-TDS, signal processing and nonlinear optics.

As a future perspective of the work conducted in this thesis, the two-wire waveguide could be improved by covering the waveguide with a polymer jacket. The polymer jacket would protect the guiding region from unwanted external impurities, protect the wires from loosening, getting dented and make the whole structure much more convenient to handle. New ways of THz signal processing could also be achieved with the design of proper waveguides. For example, metamaterials and new geometries of Bragg gratings could be coupled to the two-wire waveguide mode for modulating the THz signal. This will avoid the use of intermediate signal processing units, which can induce unwanted losses. Enhanced THz-TDS could also be envisioned for the future. For example, the tight confinement of THz radiation in between the wires provides longer interaction length for the samples to be characterizes by THz-TDS. This will enhance the spectral response of the material being studied. Finally, following an in-depth theoretical analysis of the demonstrated THz transmitter (chapter 4), further optimization could be carried out on this structure. Altogether, with the help of signal processing components and the THz transmitter, a novel THz source could be realized, where one could obtain a THz pulse with desired pulse shape and spectrum.

References

[1] P. R. Smith, D. H. Auston, and M. C. Nuss, "Subpicosecond photoconducting dipole antennas," *IEEE Journal of Quantum Electronics,* vol. 24, pp. 255-260, 1988.

[2] A. Nahata, A. S. Weling, and T. F. Heinz, "A wideband coherent terahertz spectroscopy system using optical rectification and electro-optic sampling," *Applied Physics Letters,* vol. 69, pp. 2321-2323, 1996.

[3] R. Kohler, A. Tredicucci, F. Beltram, H. E. Beere, E. H. Linfield, A. G. Davies, *et al.*, "Terahertz semiconductor-heterostructure laser," *Nature,* vol. 417, pp. 156-159, 2002.

[4] D. Banerjee, W. von Spiegel, M. D. Thomson, S. Schabel, and H. G. Roskos, "Diagnosing water content in paper by terahertz radiation," *Optics Express,* vol. 16, pp. 9060-9066, 2008.

[5] M. Naftaly, J. F. Molloy, G. V. Lanskii, K. A. Kokh, and Y. M. Andreev, "Terahertz time-domain spectroscopy for textile identification," *Applied Optics,* vol. 52, pp. 4433-4437, 2013.

[6] L. Yunfei, T. Jiajin, J. Ling, S. Shengcai, J. Biaobing, and M. Jinlong, "Study on terahertz time domain spectroscopy of pine wood nematode disease," *International Conference on Microwave Technology and Computational Electromagnetics ICMTCE*, pp. 271-275, 2009.

[7] Y.-S. Jin, G.-J. Kim and S.-G. Jeon, "Terahertz dielectric properties of polymers," *Journal of Korean Physical Society,* vol. 49, pp. 513-517, 2006.

[8] R. M. Woodward, B. E. Cole, V. P. Wallace, R. J. Pye, D. D. Arnone, E. H. Linfield, *et al.*, "Terahertz pulse imaging in reflection geometry of human skin cancer and skin tissue," *Physics in Medicine and Biology,* vol. 47, p. 3853, 2002.

[9] http://www.sp.phy.cam.ac.uk/SPWeb/research/thzcamera/WhatIsTHzImaging.htm.

[10] T. G. Phillips and J. Keene, "Submillimeter astronomy [heterodyne spectroscopy]," *Proceedings of the IEEE,* vol. 80, pp. 1662-1678, 1992.

[11] C. A. Schmuttenmaer, "Exploring dynamics in the far-infrared with terahertz spectroscopy," *Chemical Reviews,* vol. 104, pp. 1759-1780, 2004.

[12] P. R. Griffiths and J. A. D. Haseth, *Fourier transform infrared spectroscopy*. New York: Wiley, 1986.

[13] M. Naftaly and R. E. Miles, "Terahertz time-domain spectroscopy for material characterization," *Proceedings of the IEEE,* vol. 95, pp. 1658-1665, 2007.

[14] M. R. Kutteruf, C. M. Brown, L. K. Iwaki, M. B. Campbell, T. M. Korter, and E. J. Heilweil, "Terahertz spectroscopy of short-chain polypeptides," *Chemical Physics Letters,* vol. 375, pp. 337-343, 2003.

[15] A. G. Markelz, A. Roitberg, and E. J. Heilweil, "Pulsed terahertz spectroscopy of DNA, bovine serum albumin and collagen between 0.1 and 2.0 THz," *Chemical Physics Letters,* vol. 320, pp. 42-48, 2000.

[16] M. R. Leahy-Hoppa, M. J. Fitch, X. Zheng, L. M. Hayden, and R. Osiander, "Wideband terahertz spectroscopy of explosives," *Chemical Physics Letters,* vol. 434, pp. 227-230, 2007.

[17] J. F. Federici, B. Schulkin, F. Huang, D. Gary, R. Barat, F. Oliveira, *et al.*, "THz imaging and sensing for security applications—explosives, weapons and drugs," *Semiconductor Science and Technology,* vol. 20, pp. S266-S280, 2005.

[18] A. A. Gowen, C. O'Sullivan, and C. P. O'Donnell, "Terahertz time domain spectroscopy and imaging: Emerging techniques for food process monitoring and quality control," *Trends in Food Science & Technology,* vol. 25, pp. 40-46, 2012.

[19] D. Crawley, C. Longbottom, V. P. Wallace, M. Pepper, B. Cole, and D. Arnone, "Three-dimensional terahertz pulse imaging of dental tissue," *Journal of Biomedical Optics,* vol. 8, pp. 303-307, 2003.

[20] R. Huber, F. Tauser, A. Brodschelm, M. Bichler, G. Abstreiter, and A. Leitenstorfer, "How many-particle interactions develop after ultrafast excitation of an electron-hole plasma," *Nature,* vol. 414, pp. 286-289, 2001.

[21] R. A. Kaindl, M. A. Carnahan, J. Orenstein, D. S. Chemla, H. M. Christen, H.-Y. Zhai, *et al.*, "Far-infrared optical conductivity gap in superconducting MgB_2 films," *Physical Review Letters,* vol. 88, pp. 027003/1-027003/4, 2001.

[22] T. Nagatsuma, S. Horiguchi, Y. Minamikata, Y. Yoshimizu, S. Hisatake, S. Kuwano, *et al.*, "Terahertz wireless communications based on photonics technologies," *Optics Express,* vol. 21, pp. 23736-23747, 2013.

[23] R. E. Collin, *Foundations for Microwave Engineering*, Second ed. New Jersey, USA: John Wiley & Sons. Inc., 2001.

[24] Federal Communications Commission, United States Frequency Allocations: The Radio Spectrum Chart (2011).

[25] P. A. Krug, J. Chow, B. J. Eggleton, P. Hill, M. Ibsen, F. Ouellette, *et al.*, "Applications for fiber Bragg gratings in communications," in *Optical Fiber Communications(OFC '96)*, p. 116, 1996.

[26] S. Verghese, K. A. McIntosh, and E. R. Brown, "Highly tunable fiber-coupled photomixers with coherent terahertz output power," *IEEE Transactions on Microwave Theory and Techniques,* vol. 45, pp. 1301-1309, 1997.

[27] M. Van Exter and D. Grischkowsky, "Characterization of an optoelectronic terahertz beam system," *IEEE Transactions on Microwave Theory and Techniques,* vol. 38, pp. 1684-1691, 1990.

[28] G. Kozlov and A. Volkov, *Millimeter and Submillimeter Wave Spectroscopy of Solids.* Berlin: Springer-Verlag, 1998.

[29] Y.-S. Lee, *Principles of Terahertz Science and Technology.* New York: Springer, 2009.

[30] W. Shi, Y. J. Ding, N. Fernelius, and K. Vodopyanov, "Efficient, tunable, and coherent 0.18-5.27-THz source based on GaSe crystal," *Optics Letters,* vol. 27, pp. 1454-1456, 2002.

[31] K. Kawase, J.-i. Shikata, K. Imai, and H. Ito, "Transform-limited, narrow-linewidth, terahertz-wave parametric generator," *Applied Physics Letters,* vol. 78, pp. 2819-2821, 2001.

[32] K. J. Siebert, H. Quast, R. Leonhardt, T. Löffler, M. Thomson, T. Bauer, *et al.*, "Continuous-wave all-optoelectronic terahertz imaging," *Applied Physics Letters,* vol. 80, pp. 3003-3005, 2002.

[33] I. S. Gregory, W. R. Tribe, C. Baker, B. E. Cole, M. J. Evans, L. Spencer, *et al.*, "Continuous-wave terahertz system with a 60 dB dynamic range," *Applied Physics Letters,* vol. 86, pp. 204104/1-204104/3, 2005.

[34] G. W. Chantry, *Long-wave Optics* vol. 2. London: Academic Press, Inc., 1984.

[35] A. Bergner, U. Heugen, E. Bründermann, G. Schwaab, M. Havenith, D. R. Chamberlin, *et al.*, "New p-Ge THz laser spectrometer for the study of solutions: THz absorption spectroscopy of water," *Review of Scientific Instruments,* vol. 76, pp. 063110/1-063110/5, 2005.

[36] A. Maestrini, J. S. Ward, J. J. Gill, H. S. Javadi, E. Schlecht, C. Tripon-Canseliet, *et al.*, "A 540-640-GHz high-efficiency four-anode frequency tripler," *IEEE Transactions on Microwave Theory and Techniques,* vol. 53, pp. 2835-2843, 2005.

[37] http://www.longwavephotonics.com/products.

[38] E. H. Putley, "Indium Antimonide submillimeter photoconductive detectors," *Applied Optics,* vol. 4, pp. 649-657, 1965.

[39] P. Yagoubov, M. Kroug, H. Merkel, E. Kollberg, G. Gol'tsman, S. Svechnikov, *et al.*, "Noise temperature and local oscillator power requirement of NbN phonon-cooled hot electron bolometric mixers at terahertz frequencies," *Applied Physics Letters,* vol. 73, pp. 2814-2816, 1998.

[40] A. Skalare, W. R. McGrath, B. Bumble, H. G. LeDuc, P. J. Burke, A. A. Verheijen, *et al.*, "Large bandwidth and low noise in a diffusion-cooled hot-electron bolometer mixer," *Applied Physics Letters,* vol. 68, pp. 1558-1560, 1996.

[41] H. Hamster, A. Sullivan, S. Gordon, W. White, and R. W. Falcone, "Subpicosecond, electromagnetic pulses from intense laser-plasma interaction," *Physical Review Letters,* vol. 71, pp. 2725-2728, 1993.

[42] T. Löffler, F. Jacob, and H. G. Roskos, "Generation of terahertz pulses by photoionization of electrically biased air," *Applied Physics Letters,* vol. 77, pp. 453-455, 2000.

[43] T. Bartel, P. Gaal, K. Reimann, M. Woerner, and T. Elsaesser, "Generation of single-cycle THz transients with high electric-field amplitudes," *Optics Letters,* vol. 30, pp. 2805-2807, 2005.

[44] K.-Y. Kim, J. H. Glownia, A. J. Taylor, and G. Rodriguez, "Terahertz emission from ultrafast ionizing air in symmetry-broken laser fields," *Optics Express,* vol. 15, pp. 4577-4584, 2007.

[45] M. Clerici, M. Peccianti, B. E. Schmidt, L. Caspani, M. Shalaby, M. Giguère, *et al.*, "Wavelength scaling of terahertz generation by gas ionization," *Physical Review Letters,* vol. 110, pp. 253901/1-253901/5, 2013.

[46] M. Tani, S. Matsuura, K. Sakai, and S.-i. Nakashima, "Emission characteristics of photoconductive antennas based on low-temperature-grown GaAs and semi-insulating GaAs," *Applied Optics,* vol. 36, pp. 7853-7859, 1997.

[47] J. Xu and X.C. Zhang, *Introduction to THz wave photonics*. New York: Springer, 2010.

[48] P. F. Taday, I. V. Bradley, D. D. Arnone, and M. Pepper, "Using terahertz pulse spectroscopy to study the crystalline structure of a drug: A case study of the polymorphs of ranitidine hydrochloride," *Journal of Pharmaceutical Sciences,* vol. 92, pp. 831-838, 2003.

[49] E. Pickwell, A. J. Fitzgerald, B. E. Cole, P. F. Taday, R. J. Pye, T. Ha, *et al.*, "Simulating the response of terahertz radiation to basal cell carcinoma using ex vivo spectroscopy measurements," *Journal of Biomedical Optics,* vol. 10, pp. 064021/1-064021/7, 2005.

[50] J. Shan, F. Wang, E. Knoesel, M. Bonn, and T. F. Heinz, "Measurement of the frequency-dependent conductivity in sapphire," *Physical Review Letters,* vol. 90, pp. 247401/1-247401/4, 2003.

[51] P. H. Siegel, "Terahertz technology," *IEEE Transactions on Microwave Theory and Techniques,* vol. 50, pp. 910-928, 2002.

[52] J. W. Waters, "Submillimeter-wavelength heterodyne spectroscopy and remote sensing of the upper atmosphere," *Proceedings of the IEEE,* vol. 80, pp. 1679-1701, 1992.

[53] R. Mendis and D. Grischkowsky, "THz interconnect with low-loss and low-group velocity dispersion," *IEEE Microwave and Wireless Components Letters,* vol. 11, pp. 444-446, 2001.

[54] R. Mendis and D. Grischkowsky, "Undistorted guided-wave propagation of subpicosecond terahertz pulses," *Optics Letters,* vol. 26, pp. 846-848, 2001.

[55] G. Gallot, S. P. Jamison, R. W. McGowan, and D. Grischkowsky, "Terahertz waveguides," *Journal of Optical Society of America B,* vol. 17, pp. 851-863, 2000.

[56] R. W. McGowan, G. Gallot, and D. Grischkowsky, "Propagation of ultrawideband short pulses of terahertz radiation through submillimeter-diameter circular waveguides," *Optics Letters,* vol. 24, pp. 1431-1433, 1999.

[57] J. Tae-In and D. Grischkowsky, "Direct optoelectronic generation and detection of sub-ps-electrical pulses on sub-mm-coaxial transmission lines," *Applied Physics Letters,* vol. 85, pp. 6092-6094, 2004.

[58] K. Wang and D. M. Mittleman, "Metal wires for terahertz wave guiding," *Nature,* vol. 432, pp. 376-379, 2004.

[59] T.-I. Jeon, J. Zhang, and D. Grischkowsky, "THz Sommerfeld wave propagation on a single metal wire," *Applied Physics Letters,* vol. 86, pp. 161904/1-161904/3, 2005.

[60] P. Tannouri, M. Peccianti, P. L. Lavertu, F. Vidal, and R. Morandotti, "Quasi-TEM mode propagation in twin-wire THz waveguides (Invited Paper)," *Chinese Optics Letters,* vol. 9, pp. 110013/1-110013/4, 2011.

[61] R. Mendis and D. Grischkowsky, "Plastic ribbon THz waveguides," *Journal of Applied Physics,* vol. 88, pp. 4449-4451, 2000.

[62] S. P. Jamison, R. W. McGowan, and D. Grischkowsky, "Single-mode waveguide propagation and reshaping of sub-ps terahertz pulses in sapphire fibers," *Applied Physics Letters,* vol. 76, pp. 1987-1989, 2000.

[63] H. Han, H. Park, M. Cho, and J. Kim, "Terahertz pulse propagation in a plastic photonic crystal fiber," *Applied Physics Letters,* vol. 80, pp. 2634-2636, 2002.

[64] L.-J. Chen, H.-W. Chen, T.-F. Kao, J.-Y. Lu, and C.-K. Sun, "Low-loss subwavelength plastic fiber for terahertz waveguiding," *Optics Letters,* vol. 31, pp. 308-310, 2006.

[65] M. Rozé, B. Ung, A. Mazhorova, M. Walther, and M. Skorobogatiy, "Suspended core subwavelength fibers: towards practical designs for low-loss terahertz guidance," *Optics Express,* vol. 19, pp. 9127-9138, 2011.

[66] J. Harrington, R. George, P. Pedersen, and E. Mueller, "Hollow polycarbonate waveguides with inner Cu coatings for delivery of terahertz radiation," *Optics Express,* vol. 12, pp. 5263-5268, 2004.

[67] B. Bowden, J. A. Harrington, and O. Mitrofanov, "Low-loss modes in hollow metallic terahertz waveguides with dielectric coatings," *Applied Physics Letters,* vol. 93, pp. 181104/1-181104/3, 2008.

[68] C. Yeh, F. Shimabukuro, and P. H. Siegel, "Low-loss terahertz ribbon waveguides," *Applied Optics.,* vol. 44, pp. 5937-5946, 2005.

[69] A. Hassani, A. Dupuis, and M. Skorobogatiy, "Porous polymer fibers for low-loss terahertz guiding," *Optics Express,* vol. 16, pp. 6340-6351, 2008.

[70] B. Ung, A. Mazhorova, A. Dupuis, M. Rozé, and M. Skorobogatiy, "Polymer microstructured optical fibers for terahertz wave guiding," *Optics Express,* vol. 19, pp. B848-B861, 2011.

[71] M. Mbonye, R. Mendis, and D. M. Mittleman, "A terahertz two-wire waveguide with low bending loss," *Applied Physics Letters,* vol. 95, pp. 233506/1-233506/3, 2009.

[72] J. S. Melinger, N. Laman, and D. Grischkowsky, "The underlying terahertz vibrational spectrum of explosives solids," *Applied Physics Letters,* vol. 93, pp. 011102/1-011102/3, 2008.

[73] M. K. Mridha, A. Mazhorova, M. Daneau, M. Clerici, M. Peccianti, P.-L. Lavertu, *et al.*, "Low dispersion propagation of broadband THz pulses in a two-wire waveguide," *Optical Society of America Conferences, CLEO*, p. CTh1K.6, 2013.

[74] H. Pahlevaninezhad, T. E. Darcie, and B. Heshmat, "Two-wire waveguide for terahertz," *Optics Express,* vol. 18, pp. 7415-7420, 2010.

[75] A. Markov and M. Skorobogatiy, "Two-wire terahertz fibers with porous dielectric support," *Optics Express,* vol. 21, pp. 12728-12743, 2013.

[76] H. Pahlevaninezhad and T. E. Darcie, "Coupling of terahertz waves to a two-wire waveguide," *Optics Express,* vol. 18, pp. 22614-22624, 2010.

[77] X. Xin, H. Altan, A. Saint, D. Matten, and R. R. Alfano, "Terahertz absorption spectrum of para and ortho water vapors at different humidities at room temperature," *Journal of Applied Physics,* vol. 100, pp. 094905/1-094905/4, 2006.

[78] M. van Exter, C. Fattinger, and D. Grischkowsky, "Terahertz time-domain spectroscopy of water vapor," *Optics Letters,* vol. 14, pp. 1128-1130, 1989.

[79] L. Wentai, Z. Chunxi, L. Lijing, and L. Sheng, "Review on development and applications of fiber-optic sensors," *Symposium on Photonics and Optoelectronics (SOPO)*, pp. 1-4, 2012.

[80] A. Farhad, "Fiber optic health monitoring of civil structures using long gage and acoustic sensors," *Smart Materials and Structures,* vol. 14, p. S1, 2005.

[81] P. Petruzzi, C. Lowry, and P. Sivanesan, "Dispersion compensation using only fiber Bragg gratings," *IEEE Journal of Selected Topics in Quantum Electronics,* vol. 5, pp. 1339-1344, 1999.

[82] A. M. Vengsarkar, P. J. Lemaire, J. B. Judkins, V. Bhatia, T. Erdogan, and J. E. Sipe, "Long-period fiber gratings as band-rejection filters," *Lightwave Technology, Journal of,* vol. 14, pp. 58-65, 1996.

[83] K. O. Hill, B. Malo, F. Bilodeau, S. Thériault, D. C. Johnson, and J. Albert, "Variable-spectral-response optical waveguide Bragg grating filters for optical signal processing," *Optics Letters,* vol. 20, pp. 1438-1440, 1995.

[84] I. Baumann, J. Seifert, W. Nowak, and M. Sauer, "Compact all-fiber add-drop-multiplexer using fiber Bragg gratings," *Photonics Technology Letters, IEEE,* vol. 8, pp. 1331-1333, 1996.

[85] L. M. Rivas, S. Boudreau, Y. Park, R. Slavík, S. LaRochelle, A. Carballar, *et al.*, "Experimental demonstration of ultrafast all-fiber high-order photonic temporal differentiators," *Optics Letters,* vol. 34, pp. 1792-1794, 2009.

[86] M. H. Asghari and J. Azana, "On the design of efficient and accurate arbitrary-order temporal optical integrators using fiber Bragg gratings," *Lightwave Technology, Journal of,* vol. 27, pp. 3888-3895, 2009.

[87] M. R. Fernández-Ruiz, M. Li, M. Dastmalchi, A. Carballar, S. LaRochelle, and J. Azaña, "Picosecond optical signal processing based on transmissive fiber Bragg gratings," *Optics Letters,* vol. 38, pp. 1247-1249, 2013.

[88] http://en.wikipedia.org/wiki/File:Fiber_Bragg_Grating-en.svg.

[89] Z. Jian, J. Pearce, and D. M. Mittleman, "Defect modes in photonic crystal slabs studied using terahertz time-domainspectroscopy," *Optics Letters,* vol. 29, pp. 2067-2069, 2004.

[90] A. Bingham, Y. Zhao, and D. Grischkowsky, "THz parallel plate photonic waveguides," *Applied Physics Letters,* vol. 87, pp. 051101/1-051101/3, 2005.

[91] Z. Jian, J. Pearce, and D. M. Mittleman, "Two-dimensional photonic crystal slabs in parallel-plate metal waveguides studied with terahertz time-domain spectroscopy," *Semiconductor Science and Technology,* vol. 20, pp. S300-S306, 2005.

[92] Y. Zhao and D. Grischkowsky, "Terahertz demonstrations of effectively two-dimensional photonic bandgap structures," *Optics Letters,* vol. 31, pp. 1534-1536, 2006.

[93] Y. Zhao and D. Grischkowsky, "2-D Terahertz metallic photonic crystals in parallel-plate waveguides," *IEEE Transactions on Microwave Theory and Techniques,* vol. 55, pp. 656-663, 2007.

[94] S. S. Harsha, N. Laman, and D. Grischkowsky, "High-Q terahertz Bragg resonances within a metal parallel plate waveguide," *Applied Physics Letters,* vol. 94, pp. 091118/1-091118/3, 2009.

[95] G. Yan, A. Markov, Y. Chinifooroshan, S. M. Tripathi, W. J. Bock, and M. Skorobogatiy, "Low-loss terahertz waveguide Bragg grating using a two-wire waveguide and a paper grating," *Optics Letters,* vol. 38, pp. 3089-3092, 2013.

[96] H. Lene Vestergaard, S. E. Harris, D. Zachary, and H. B. Cyrus, "Light speed reduction to 17 metres per second in an ultracold atomic gas," *Nature,* vol. 397, pp. 594-598, 1999.

[97] M. S. Bigelow, N. N. Lepeshkin, and R. W. Boyd, "Observation of ultraslow light propagation in a ruby crystal at room temperature," *Physical Review Letters,* vol. 90, pp. 113903/1-113903/4, 2003.

[98] M. S. Bigelow, N. N. Lepeshkin, and R. W. Boyd, "Superluminal and slow light propagation in a room-temperature solid," *Science,* vol. 301, pp. 200-202, 2003.

[99] M. González-Herráez, K.-Y. Song, and L. Thévenaz, "Optically controlled slow and fast light in optical fibers using stimulated Brillouin scattering," *Applied Physics Letters,* vol. 87, pp. 081113/1-081113/3, 2005.

[100] Y. Okawachi, M. S. Bigelow, J. E. Sharping, Z. Zhu, A. Schweinsberg, D. J. Gauthier, *et al.*, "Tunable all-optical delays via Brillouin slow light in an optical fiber," *Physical Review Letters,* vol. 94, pp. 153902/1-153902/4, 2005.

[101] Z. Shi, A. Schweinsberg, J. E. Vornehm Jr, M. A. Martínez Gámez, and R. W. Boyd, "Low distortion, continuously tunable, positive and negative time delays by slow and fast light using stimulated Brillouin scattering," *Physics Letters A,* vol. 374, pp. 4071-4074, 2010.

[102] F. Xia, L. Sekaric, M. O'Boyle, and Y. Vlasov, "Coupled resonator optical waveguides based on silicon-on-insulator photonic wires," *Applied Physics Letters,* vol. 89, pp. 041122/1-041122/3, 2006.

[103] Q. Gan, Z. Fu, Y. J. Ding, and F. J. Bartoli, "Ultrawide-bandwidth slow-light system based on THz plasmonic graded metallic grating structures," *Physical Review Letters,* vol. 100, pp. 256803/1-256803/4, 2008.

[104] Q. Gan, Y. Gao, K. Wagner, D. Vezenov, Y. J. Ding, and F. J. Bartoli, "Experimental verification of the rainbow trapping effect in adiabatic plasmonic gratings," *Proceedings of the National Academy of Sciences,* vol. 108, pp. 5169-5173, 2011.

[105] T. F. Krauss, "Slow light in photonic crystal waveguides," *Journal of Physics D: Applied Physics,* vol. 40, pp. 2666-2670, 2007.

[106] T. Baba, "Slow light in photonic crystals," *Nature Photonics,* vol. 2, pp. 465-473, 2008.

[107] J. T. Mok, C. M. de Sterke, I. C. M. Littler, and B. J. Eggleton, "Dispersionless slow light using gap solitons," *Nature Physics,* vol. 2, pp. 775-780, 2006.

[108] W. He, M. Terrel, F. Shanhui, and M. Digonnet, "Sensing with slow light in fiber Bragg gratings," *IEEE Sensors Journal,* vol. 12, pp. 156-163, 2012.

[109] R. W. Boyd, "Material slow light and structural slow light: similarities and differences for nonlinear optics [Invited]," *Journal of Optical Society of America B*, vol. 28, pp. A38-A44, 2011.